Quantification of the insulin response in rat L6 skeletal muscle cells

by

Klarissa Shaw

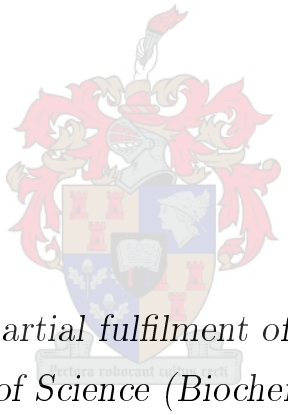

Thesis presented in partial fulfilment of the requirements for the degree of Master of Science (Biochemistry) in the Faculty of Biochemistry at Stellenbosch University

Supervisor: Prof. JL. Snoep

Co-supervisor: Dr DD. van Niekerk

March 2020

Declaration

By submitting this thesis electronically, I declare that the entirety of the work contained therein is my own, original work, that I am the sole author thereof (save to the extent explicitly otherwise stated), that reproduction and publication thereof by Stellenbosch University will not infringe any third party rights and that I have not previously in its entirety or in part submitted it for obtaining any qualification.

Date: March 2020 .....

Abstract

Quantification of the insulin response in rat L6 skeletal muscle cells

K. Shaw

Department of Biochemistry,
University of Stellenbosch,
Private Bag X1, Matieland 7602, South Africa.

Thesis: MSc (Biochemistry)

March 2020

Mathematical models can help us to understand complex molecular mechanisms underlying diseases. There is a lack of these types of models describing the cellular processes involved in conditions such as insulin resistance and Type 2 diabetes (T2D). Therefore, this study aimed to quantify the reference state of the insulin signalling pathway for the construction of a mathematical model describing the dynamics of the pathway intermediates. This model will serve as a comparison for a model describing the diabetic state. Western blot analysis was used to quantify the phosphorylation states of Akt Ser^{473} and Thr^{308} at varying concentrations of insulin and over time, with or without insulin. The glucose transporter, GLUT4, activity was also investigated at different concentrations of insulin. These data were used in the construction of a model for the reference state. Ordinary differential equations (ODEs) were derived to describe the dynamics of Akt over time. Steady state constraints were used to fit the dose response for Akt and made it possible to estimate a dephosphorylation/phosphorylation ratio. The estimated ratio was used to determine if the model could describe the time course data. A similar analysis was done for GLUT4. The model was able to accurately describe the phosphorylation

and dephosphorylation dynamics of the Akt Ser^{473} and Thr^{308} site. In order to determine the link between insulin signalling and glucose transport, transport activity was plotted against Akt phosphorylation and the model was fitted to this data. The fit for both the Ser^{473} and Thr^{308} site did not differ. We found that the model predictions correlated quite well with the experimental data despite the lack of data on intermediates between insulin and Akt.

Uittreksel

Kwantifisering van die insulienrespons in rats L6-skeletspierselle

K. Shaw

Departement Biochemie,
Universiteit van Stellenbosch,
Privaatsak X1, Matieland 7602, Suid Afrika.

Tesis: MSc (Biochemie)

Maart 2020

Wiskundige modelle kan ons help om komplekse molekulêre meganismes onderliggend aan siektes te verstaan. Daar is 'n gebrek aan hierdie tipe modelle wat die sellulêre prosesse beskryf wat betrokke is by toestande soos insulienweerstandigheid en Tipe 2 diabetes (T2D). Daarom het hierdie studie ten doel gehad om die verwysingstoestand van die insulien seinepad te kwantifiseer vir die konstruksie van 'n wiskundige model wat die dinamika van die tussengangerselprodukte beskryf. Hierdie model sal as vergelyking dien vir 'n model wat die diabetiese toestand beskryf. Western blot analise is gebruik om die fosforileringstoestande van Akt Ser^{473} en Thr^{308} te kwantifiseer by verskillende konsentrasies insulien en met verloop van tyd, met of sonder insulien. Die glukosetransporter, GLUT4, is ook by verskillende konsentrasies insulien ondersoek. Hierdie is gegewens gebruik vir die konstruksie van 'n model vir die verwysingstoestand. Gewone differensiaalvergelykings (ODE's) is afgelei om die dinamika van Akt oor tyd te beskryf. Gereelde beperkings is gebruik om by die dosisrespons vir Akt te pas en het dit moontlik gemaak om 'n defosforilering / fosforilasie-verhouding te skat. Die beraamde verhouding is gebruik om te bepaal of die model die tydsverloopdata kon beskryf. 'n Soortgelyke

analise is vir GLUT4 gedoen. Die model kon die fosforilering en defosforilering dinamika van die Akt Ser^{473} en Thr^{308} akkuraat beskryf. Ten einde die verband tussen insulien seine en glukose vervoer te bepaal, is vervoeraktiwiteit teen Akt fosforilering geplot en die model was op hierdie date gepas. Die pas vir beide die Ser^{473} en Thr^{308} verhouding met GLUT4 het nie verskil nie. Ons het gevind dat die modelvoorspellings redelik goed met die eksperimentele data gekorreleer het, ondanks die gebrek aan data oor tussenprodukte tussen insulien en Akt.

Acknowledgements

I would like to express my sincere gratitude to the following people and organisations ...

- My supervisor, Prof. JL Snoep, for your patience, guidance and understanding through difficult times.
- My co-supervisor, Dr. DD van Niekerk, thank you that I could always rely on you when needed.
- SARCHI for funding.
- Mr. Arrie Arends, our lab manager, for always putting the students first. We would not be able to do this without you.
- Dr. Theresa Kouril this masters would not have been possible without you.
- Stefan Kuhn, thank you for being a great mentor and friend.
- Everyone in the MSB lab, especially Morne, Clara, Christoff, Lauren and Cobus.
- My family and friends
- Justin, for all your love and support.

Dedications

Hierdie tesis word opgedra aan my ouers, Kevin en Carma, en suster Natalia. Dankie vir al julle liefde en ondersteuning.

Contents

Declaration i

Abstract ii

Uittreksel iv

Acknowledgements vi

Dedications vii

Contents viii

List of Figures x

List of Tables xiv

Nomenclature xv

1 Introduction 1

2 Literature Review 5

2.1 Introduction 5

2.2 The Insulin Signalling Pathway 7

2.3 Critical nodes in signalling pathways 10

2.4 Insulin resistance and insulin signalling 15

2.5 L6 muscle cells as a model system 17

2.6 Systems Biology 18

3 Materials and Methods 22

4 Results **25**
4.1 Introduction 25
4.2 Optimization of experimental procedures 26
4.3 Measuring Akt Ser^{473} ,Thr^{308} phosphorylation dynamics and GLUT4 transporter activity 30
4.4 Modelling the phosphorylation dynamics of Akt Ser^{473} and Thr^{308} 35

5 Discussion, Future work and Conclusions **43**
5.1 Discussion 43
5.2 Conclusion 47

A Appendix **48**

List of References **50**

List of Figures

1.1 **An illustration of the insulin-signalling pathway.** This scheme illustrates the series of phosphorylation reactions initialised by the binding of insulin to the IR and ending with translocation of the GLUT4 transporter to the cell membrane. The solid arrows represents activation and the red dot dashed arrows represent inhibition. The black dotted lines represent movement of the GLUT4 vesicle to the membrane and glucose across the membrane. The full names of the proteins can be found in the Nomenclature. This figure was created by the author. 4

2.1 **The stimulatory and inhibitory effects of insulin on processes carried out by different tissues.** This image was created in Wolfram Mathematica® using the AnatomyPlot3D function. . . 6

2.2 **Schematic of the insulin signalling pathway without insulin bound (a) and insulin bound (b)**. Insulin (green) binds to IR (blue) which leads to a conformational change in IR allowing transautophosphorylation. Phosphorylated IR then phosphorylates IRS (yellow) which leads to the recruitment of the regulatory subunit of PI3K (purple) to the membrane. This allows for the catalytic subunit of PI3K to phosphorylate lipids in the membrane, leading to recruitment and downstream phosphorylation of Akt (orange). Phosphorylated Akt leads to the recruitment of GSVs (sphere containing cylinders(GLUT4) to the membrane where it docks and fuses with the membrane leading to increasing concentrations of GLUT4 (grey cylinders) at the membrane, allowing increased glucose uptake. This image was created by the author in Wolfram Mathematica using the 3DPlot function. 9

4.1 **Cell culture photos of L6 muscle cells.** Figures (a) and (b) are differentiated L6 muscle fibers that have started lifting off the culture dishes. It can be seen that the fibers appear to be thin and more elongated with notable quantities of cell debris clearly visible. Figure (c) shows growing L6 myoblasts almost ready for differentiation. Figure (d) shows differentiated L6 myofibers, which are formed when myoblasts align and fuse to form thick and long muscle fibers. 27

4.2 **Passaging protocol for L6 myoblasts.** L6 myoblasts were seeded from freezerstock into a T25 flask, once the cells were 70-80% confluent they were passaged into one T75 flask. When the T75 flask reached the same confluence it was split into three T75 flasks. Each of the three T75 flasks were passaged into two T75 flasks, reulting in six T75 flasks. Once these six flasks were 70-80% confluent, they were each passaged into five 100mm cultures dishes respectively. . . 28

4.3 **Time dependent phosphorylation of Akt.** Cells were incubated with 100nM insulin and harvested at different timepoints. Each sample was probed with specific Akt Ser^{473} , Thr^{308} and total antibody. The antibody signal was plotted against time for Akt Ser^{473} (a), Akt Thr^{308} (b) and Akt total (c). Results are means of three experiments ± SE and normalised to the 30min timepoint. . . 31

4.4 **Time dependent dephosphorylation of Akt.** Cells were incubated with 100nM insulin for 30min after which the insulin was removed at different timepoints and harvested. Each sample was probed with specific Akt Ser^{473} and Thr^{308} antibodies as well as with a total Akt antibody. The antibody signal was plotted against time for Akt Ser^{473} (a), Akt Thr^{308} (b) and Akt total (c). Results are means of three experiments ± SE and normalised to the 1min time point. 32

4.5 **Dose dependent phosphorylation of Akt.** Cells were incubated with various insulin concentrations and harvested after 30min. Each sample was probed with specific Akt Ser^{473} and Thr^{308} antibodies as well as with a total Akt antibody. The antibody signal was plotted against time for Akt Ser^{473} (a), Akt Thr^{308} (b) and Akt total (c). Results are means of three experiments ± SE and normalised to the 100nM insulin concentration. 33

4.6 **GLUT4 transport activity stimulated with 1nM and 100nM insulin for 30min.** Results are means of three experiments ± SE. Between the control sample (not stimulated with insulin) and the sample stimulated with 1nM insulin there is a 1.46-fold induction ($P<0.05$*). Similarly there is a 1.91-fold ($P<0.05$*) induction between the sample stimulated with a 100nM insulin and the control. It was also determined that there was a 1.29-fold ($P<0.05$*) increase between the sample stimulated with 1nM and 100nM insulin. (*t-test: Two-Sample Assuming Equal Variances) 34

4.7 **Reaction scheme of the phosphorylation of Akt used for the derivation of kinetic equations.** 36

4.8 **Model fit to Akt Ser^{473} an Thr^{308} phosphorylation as a function of insulin.** Western blot analysis was used to quantify the phosphorylation levels for both the Ser^{473} and Thr^{308} site. Cells were incubated for 30min with the respective concentrations and values were normalized to 100nM insulin, which was considered steady state phosphorylation. Eq. 4.4.4 was fitted to experimental data for Ser^{473} and Thr^{308} . Data was normalised to their respective total. 38

4.9 **Phosphorylation and dephosphorylation data for the Ser^{473} (a) and Thr^{308} (b) site shown with the modelfit.** The data was obtained via western blot analyses by stimulating myofibers with a 100nm insulin for the respective time points and then washing away insulin to determine the dephosphorylation. The data is shown in blue with the modelfit shown as a blackcurve. 39

4.10 **Glucose transport activity as a function of Akt Ser^{473} (a) and Thr^{308} (b) phosphorylation when stimulated with insulin.** Cells were stimulated with various concentrations of insulin for 30min, Akt Ser^{473} and Thr^{308} phosphorylation were measured via western blot analysis. The phosphorylation levels were normalised to the phosphorylation level obtained with a 100nM insulin. A two-second radiolabelled glucose assay was used to determine the glucose transporter activity. 42

List of Tables

2.1 **Various IRS isoforms and their expression and functions.** . 12
2.2 **Various isoforms of PI3K and their functions.** 13

3.1 **A summary of primary- and secondary antibodies used during western blot analyses** 24

4.1 **Summary of L6 culturing conditions:** 29
4.2 **Kinetic parameters for the steady state rate equations.** Eq. 4.4.10 was fitted to the experimental dose response data for $aktSp(t)$ and $aktTp(t)$ 39

Nomenclature

AS160	Akt substrate of 160kDa
DMEM	Dulbecco's modified eagles medium
ERK	Extracellular Receptor Kinase
FBS	Fetal bovine serum
GLUT	Glucose transporter
EFGR	Epidermal growth factor receptor
HS	Horse serum
IGF1R	Insulin-like growth factor 1
IP7	Diphosphoinositol pentakisphosphate
IR	Insulin receptor
IRR	IR-related receptor
IRS	Insulin receptor substrate
GAP	GTPase-activating protein
Grb10	Growth factor receptor-bound protein 10
KO	Knockout
MAPK	Mitogen-activated protein kinase
mTORC2	mammalian target of rapamycin complex 2
NF	Nuclear factor

ODE	Ordinary differential equations
PBS	Phosphate buffered saline
PC1	Plasma cell membrane glycoprotein-1
PDE	Partial differential equations
PDK1	Phosphoinositide-dependent kinase 1
PH	Pleckstrin homology
PHLPP	PH-domain leucine-rich repeat protein phosphatase
PI3K	Phosphatidylinositol 3' kinase
PI	Phosphoinositide
PIP_2	Phosphatidylinositol 4,5-bisohosphate
PIP_3	Phosphatidylinositol (3,4,5)-triphosphate
PKB(Akt)	Protein kinase B
PKC	Protein kinase C
PP2A	Protein phosphatase-2A
PTB	Phosphotyrosine binding
PTEN	Phosphatase and tensin homolog
PTP	Protein tyrosine phosphatase
PTP1B	Protein tyrosine phosphatase 1B
RBM	Rule-based models
RSK	Ribosomal s6 kinase
RTKs	Receptor tyrosine kinases
SH2	Src Homology 2
SOCS	Supressor of cytokine signalling

T2D	Type 2 diabetes
TBC1D1	TBC1 domain family member 1
TRB3	Tribbles-3

Chapter 1

Introduction

Type 2 diabetes (T2D) is a metabolic disease that negatively impacts the health of many individuals worldwide. It accounts for 90-95% of diabetes cases [1] and the World Health Organization (WHO) reported 1.5 million deaths caused by diabetes in 2012 and in 2014 it was estimated that 422 million people suffer from diabetes [2]. Unlike Type 1 diabetes, which is usually caused by an autoimmune disorder that attacks pancreatic β-cells, T2D is thought to be the result of insulin resistance (often associated with obesity) [1]. This disease is characterised by glucose intolerance, hyperinsulinemia and insulin resistance in peripheral tissues such as skeletal muscle, adipose tissue and the liver [3]. When left untreated T2D can cause irreversible damage to organs and puts individuals affected by this condition at higher risk for strokes, cardiovascular disease, kidney failure, vision loss, nerve damage and many other complications [4]. Typically T2D is treated with lifestyle changes such as diet and exercise as well as drugs like metformin which helps regulate blood glucose levels [5]. Metformin has been used for over 50 years to treat T2D and is known to lower the production of glucose and increase glucose utilization. However, the exact mechanism whereby metformin elicits these effects remains poorly understood, and this drug is not without its side effects [6]. Lifestyle changes and drugs are helpful to reduce blood glucose levels to normoglycemia, but cannot reverse the damage that has already been done to tissues and organs.

It is necessary to investigate the cellular mechanisms underlying conditions such as insulin resistance and T2D to understand the extent of the metabolic dysfunction. There are three main tissues implicated in T2D, skeletal muscle,

adipocytes and the liver. Of these three, skeletal muscle is responsible for $\pm$ 75% of insulin-dependent glucose uptake [7] and is therefore important for maintaining glucose homeostasis. To understand how insulin regulates glucose uptake, further investigation into the dynamics of the insulin signalling pathway is required. Dysregulation in this pathway can lead to insulin resistance and T2D. There is still uncertainty as to the precise molecular mechanisms underlying these medical conditions. The insulin signalling pathway is complex with a large degree of crosstalk between the signalling intermediates. This is further complicated considering that each of these proteins are phosphorylated and dephosphorylated at multiple sites in response to insulin and various components from other signalling pathways (Fig. 1.1). This complexity hinders progress when it comes to understanding diseases like T2D. Mathematical models can help us to elucidate such complex systems, to identify new drug targets and to test new drugs.

The structure of the insulin signalling pathway is well known, however, there is a lack of kinetic mechanistic models describing the dynamics of this pathway. This project forms part of a larger goal to have a mathematical model for Type 2 diabetes that consists of three compartments namely: insulin signalling, glucose transport, and glucose metabolism. To achieve this we first need to establish the dynamics of the reference state, which in this case refers to cells that are not insulin resistant or diabetic. Although the components of the pathway are well known, the dynamic and kinetic behaviour still needs to be elucidated. There is a lack of data in literature that describes the dose and time dependent behaviour of the pathway intermediates. To understand what complications arise on a molecular level during insulin resistance and T2D we first need to determine the behaviour of the pathway under healthy physiological conditions after which we will have a model to compare the diabetic state to.

This led us to the following research question:

1. Can we construct a mathematical model that describes the insulin signalling pathway dynamics and link this to glucose transport?

The aim of this thesis is therefore to come to a quantitative description of the insulin signalling pathway and its link to glucose transport induction of the reference state. In this project rat skeletal muscle cells are used but the techniques and analyses can be extended to other cell lines in future studies. This reference state will serve as a control in a follow up study in insulin insensitive cells, to determine where changes have occurred, leading to the reduced insulin response. To achieve this aim the following objectives were set:

- Determine the phosphorylation levels of key intermediates in the insulin signalling pathway at varying insulin concentrations.
- Determine the phosphorylation and dephosphorylation of key intermediates in the insulin signalling pathway upon insulin stimulation/ removal over time.
- Determine the glucose transport dynamics at varying doses of insulin as well as over time with the addition or removal of insulin.
- Construct a mathematical model that describes the reactions of the insulin signalling pathway.

The thesis is structured as follows: Firstly in Chapter 2, I will be discussing the important literature related to T2D and mathematical modelling. Chapter 3 follows with the methodologies used to perform the experiments presented in this thesis. The results are presented in Chapter 4, starting with an optimization section after which the results of the phosphorylation and glucose transporter experiments are presented. Chapter 4 ends with the model description and results obtained from the model. Chapter 5 serves as a general discussion and conclusion chapter.

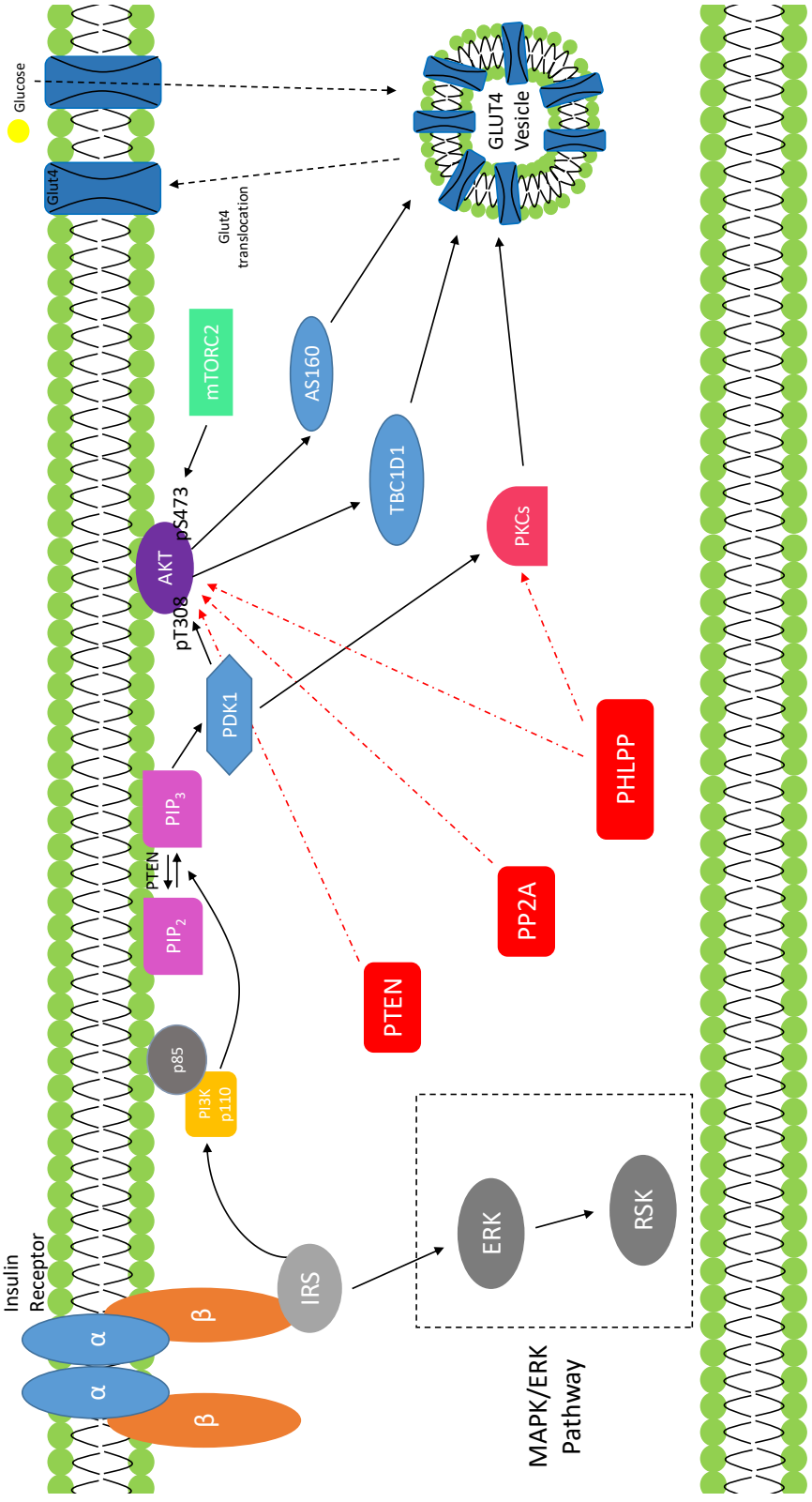

Figure 1.1: **An illustration of the insulin-signalling pathway.** This scheme illustrates the series of phosphorylation reactions initialised by the binding of insulin to the IR and ending with translocation of the GLUT4 transporter to the cell membrane. The solid arrows represents activation and the red dot dashed arrows represent inhibition. The black dotted lines represent movement of the GLUT4 vesicle to the membrane and glucose across the membrane. The full names of the proteins can be found in the Nomenclature. This figure was created by the author.

Chapter 2

Literature Review

2.1 Introduction

Insulin is the most important hormone for maintaining glucose homeostasis in the body [8]. When blood glucose levels rise, insulin is secreted from the pancreatic beta cells into the blood stream. The secretion of insulin stimulates the uptake of glucose primarily into the muscle and adipose tissue, where it is stored as glycogen and triglycerides respectively (see Fig. 2.1) [8]. Simultaneously, insulin also acts on the liver to prevent it from producing more glucose by inhibiting processes such as gluconeogenesis and glycogenolysis, which further prevents increases in blood glucose levels after a meal [8]. However, when target tissues fail to respond to normal levels of circulating insulin a condition known as insulin resistance develops [9]. Insulin resistance is considered the precursor to more serious diseases such as T2D. One of the first abnormalities observed during insulin resistance is the decrease in insulin dependent glucose uptake by striated muscle tissue and adipocytes, as well as the decrease in the ability of insulin to suppress glucose production by the liver [9]. The onset of T2D is characterised by consistently high blood glucose concentrations, which persist despite moderate to high levels of insulin present in the bloodstream [8]. As T2D progresses, the ability of the pancreatic beta cells to secrete insulin is exhausted and this leads to low levels of insulin in blood circulation, calling for exogenous insulin to be administered [8]. Due to the blood glucose levels in T2D patients remaining persistently high over many years, clinical complications such as cardiovascular disease, retinopathy, neuropathy and nephropathy develop, contributing to the morbidity and mortality of this disease [8]. The

high incidence of T2D along with its serious complications, makes it vital to understand the molecular mechanisms of insulin dependent glucose transport as well as insulin resistance [8]. In this literature review I will focus on the various components of the insulin signalling pathway and how these components interact with one another. The effect of insulin resistance on this pathway will also be discussed as well as why L6 rat skeletal muscle cells serve as a model system for studying the insulin signalling pathway. Finally, a section on systems biology will be included reviewing some mathematical models that describe the insulin signalling pathway.

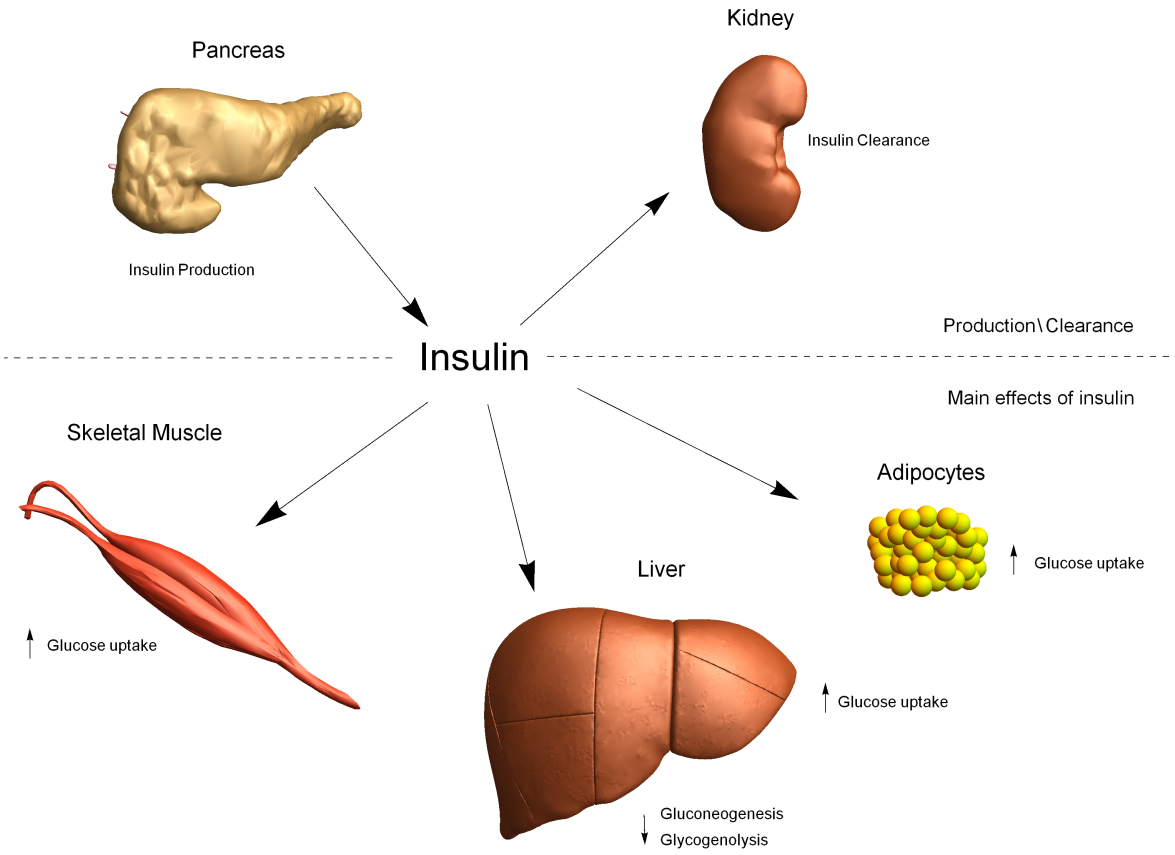

Figure 2.1: **The stimulatory and inhibitory effects of insulin on processes carried out by different tissues.** This image was created in Wolfram Mathematica® using the AnatomyPlot3D function.

2.2 The Insulin Signalling Pathway

The binding of insulin to membrane-bound receptor proteins initiates the insulin signalling pathway in mammalian cells (see Fig. 2.2). These receptors are tetramers, which consist of extracellular (two α-subunits) and transmembrane (two β-subunits) monomeric components [10]. Insulin binds to the α-subunit, which activates the intrinsic kinase activity of the β-subunit. This leads to one β-subunit tyrosine, phosphorylating an adjacent β-subunit (intramolecular transautophosphorylation) [8]. The insulin receptor substrate (IRS) contains a phosphotyrosine binding (PTB) module that interacts with phosphorylated IR, which then phosphorylates IRS on various tyrosine residues [11].

Regulatory subunits such as p85 with Src Homology 2 (SH2) use the phosphorylated tyrosine residues on IRS as docking sites. This regulatory subunit exists as a dimer in the cytosol and is composed of a regulatory subunit, p85 and a catalytic subunit p110α.p85 is the most important regulatory subunit of Type IA phosphatidylinositol 3' kinase (PI3K) [12]. Recruitment of the regulatory subunit to the membrane allows the catalytic subunit p110α to catalyse the phosphorylation of phosphoinositide (PI) lipids in the 3' position of the inositol ring. This reaction allows for the phosphorylation of phosphatidylinositol 4,5-bisphosphate (PIP_2) to form the second lipid messenger phosphatidylinositol (3,4,5)-triphosphate (PIP_3) [10]. The phosphorylation of the PIP proteins allows for the recruitment and downstream activation of Akt also known as Protein Kinase B (PKB). Proteins containing an N-terminal pleckstrin homology (PH) domain, such as Akt, have a high infinity for PIP_3 [13].

The recruitment of Akt via PIP_3 to the membrane allows for a conformational change in Akt which leads to the phosphorylation of the Thr^{308} residue which is situated in the activation segment of Akt. Phosphorylation of the Thr^{308} site is facilitated through a membrane-localized 3-phosphoinositide-dependent kinase 1 (PDK1) leading to partial activation of Akt [13]. Full activation of Akt is achieved by phosphorylation of Ser^{473} site, which is situated in the hydrophobic motif, through mammalian target of rapamycin complex 2 (mTORC2) [14]. A GTPase-activating protein (GAP) (Akt substrate of 160kDa (AS160)) is activated by Akt downstream. AS160 contains a GTPase-activating domain for a Rab. Rab proteins have been identified to be involved

in vesicle trafficking [15]. GLUT4 is a glucose transporter responsible for insulin stimulated glucose uptake, and is known to be arranged in vesicles. Phosphorylated AS160 therefore allows GLUT4 containing vesicles (GSVs) to translocate to the plasma membrane [13] which then fuses with the membrane to facilitate glucose transport.

2.2.1 Insulin

In healthy individuals plasma glucose concentrations can vary between 4 and 7 mM, even during periods of feeding and fasting. This narrow concentration range is regulated by different processes occurring within the body, including absorption of glucose in the intestine, production of glucose by the liver as well as the metabolism and uptake of glucose by peripheral tissues [7]. Blood glucose homeostasis is primarily regulated by insulin which represses glucose production in the liver, and stimulates glucose uptake in muscle and fat tissues [7, 16]. Insulin also stimulates protein synthesis in the muscle, fatty acid uptake in adipose tissue and glucose utilization and triglyceride synthesis in the liver. In addition, it supresses glucose synthesis and inhibits lipolysis in the liver and adipose tissue, respectively [16, 17]. Energy storage and utilisation is increased by insulin via GLUT4. The increase in glucose uptake is due to the increasing levels of GLUT4 at the membrane and not an increase of intrinsic GLUT4 activity [18]. For this reason, insulin is thought to be one of the most important negative regulators of its own signalling. Furthermore, it has been shown that if insulin concentration in the blood stays consistently high, also known as hyperinsulinemia, IR internalises and undergoes lysosomal degradation or is recycled back to the membrane [19], leading to a decrease in insulin signalling. This is thought to be the basis of the concept that hyperinsulinemia and insulin resistance are associated. This can be promptly reversed through fasting, allowing plasma insulin levels to fall [16]. Insulin carries out essential functions within the body and the cascade of signals involved in these functions include many intermediates with many interactions, therefore it is important to be able to identify critical nodes in these signalling cascades.

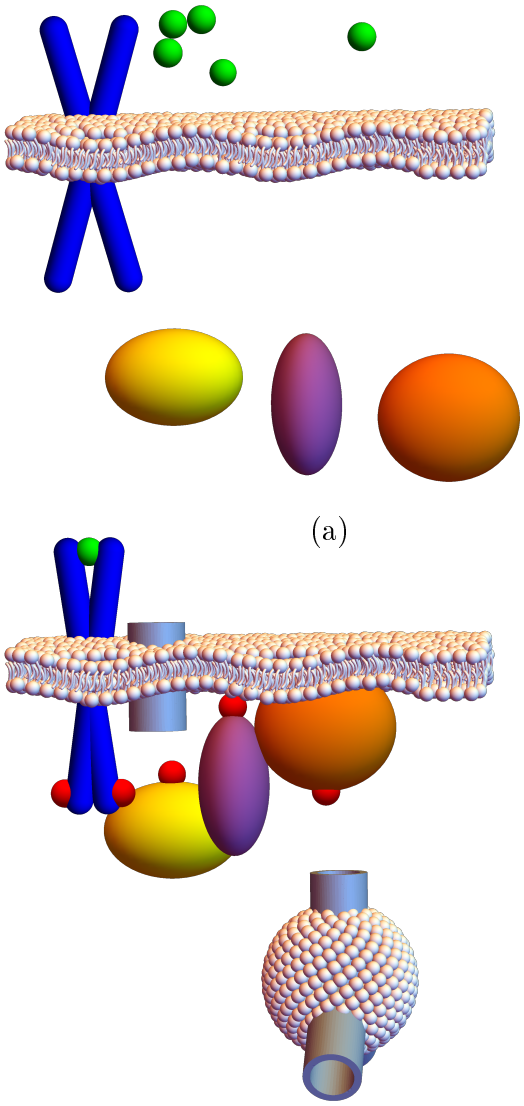

(a)

(b)

Figure 2.2: **Schematic of the insulin signalling pathway without insulin bound (a) and insulin bound (b)**. Insulin (green) binds to IR (blue) which leads to a conformational change in IR allowing transautophosphorylation. Phosphorylated IR then phosphorylates IRS (yellow) which leads to the recruitment of the regulatory subunit of PI3K (purple) to the membrane. This allows for the catalytic subunit of PI3K to phosphorylate lipids in the membrane, leading to recruitment and downstream phosphorylation of Akt (orange). Phosphorylated Akt leads to the recruitment of GSVs (sphere containing cylinders(GLUT4) to the membrane where it docks and fuses with the membrane leading to increasing concentrations of GLUT4 (grey cylinders) at the membrane, allowing increased glucose uptake. This image was created by the author in Wolfram Mathematica using the 3DPlot function.

2.3 Critical nodes in signalling pathways

Taniguchi *et al.* [20] proposes three criteria for a signalling intermediate to be classified as an essential mediator or a 'critical node'. The first criteria states that the node should constitute more than one isoform of a protein and that these dictate the receptor-mediated signal. In addition, these isoforms should fulfil unique biological functions to introduce a degree of divergence to the signalling pathway. Secondly, the possible critical node has to be governed by positive and negative feedback systems. The last criteria is that the potential critical node needs to act as a point for crosstalk between different signalling pathways. Taniguchi et al. [20] used the insulin signalling pathway as an example for this analysis and identified three critical nodes that suit the above mentioned criteria. These nodes are of the IR and IRS, P13K and lastly Akt (Fig. 2.2). Each one of these nodes will be discussed in detail below as well as one of the downstream mediators of Akt, namely GLUT4.

2.3.1 IR and IRS

The IR is a tetrameric protein with two extracellular α and two intracellular β- subunits. The IR forms part of a subfamily of receptor tyrosine kinases (RTKs), which also includes the insulin-like growth factor 1 receptor (IGF1R) and IR-related receptor (IRR) [21]. IR acts as a classical allosteric enzyme in which the tyrosine-kinase activity intrinsic to the β-subunit is inhibited by the α- subunit. This inhibition can be lifted when insulin binds to the α-subunit or the subunit is removed by genetic deletion or proteolysis, thereby activating the kinase activity of the β-subunit [22]. Initial activation of β-subunits allows for the transphosphorylation of the β- subunits, inducing a conformational change which further increases its kinase activity [20]. Two isoforms of IR exist, namely IR_A and IR_B. The more metabolically active isoform, IR_A, functions in the foetus as a growth-promoting isoform, while IR_B on the other hand is less active but is predominantly expressed in adult liver [23]. Both isoforms are expressed in the liver, muscle- and adipose tissue, but IR_B is more predominantly expressed than IR_A[24].

Eleven intracellular substrates have been identified for IR and IGF1R, with IRS constituting six of these substrates (summary in Table 2.1) [20]. Proteins that contain an SH2 domain use the phosphorylated tyrosine residues on IRS

as docking sites, for example, adapter proteins such as p85 the regulatory subunit of PI3K. Binding of substrates to adapter proteins can influence their subcellular location as well as their activity [7]. The homologs of IRS can have different functions depending on the subcellular localisation, different tissue distribution as well as intrinsic activity of these proteins [16]. For example, studies in mice involving gene knockouts (KO) have given clarity to the functions of the different IRS isoforms. Araki et al. [25] showed that IRS1 KO mice have impaired insulin action in muscle and exhibit growth retardation, however show normal glucose tolerance, whereas IRS2 KO mice displayed abnormalities regarding insulin signalling in the liver [26]. IRS1 and IRS2 KOs in pre-adipocytes lead to defects in differentiation and disruption of insulin stimulated glucose transport [27, 28]. IRS1 is necessary for glucose metabolism and myoblast differentiation in skeletal muscle cells, whereas IRS2 is crucial for ERK activation and lipid metabolism [29, 30]. IRS3 and IRS4 exhibit limited tissue distribution. IRS3 is the most abundant in rodents in lung, adipocyte and liver tissue. Humans lack IRS3, as it is expressed as a pseudogene where no product is produced [10, 16]. IRS3 KO mice do not seem to possess abnormalities, but when combined with IRS1 KO exhibit extreme defects in adipogenesis [31]. IRS4 is present in various tissues, such as brain, heart, kidney, liver and skeletal muscle. IRS4 KO mice did not have any severe defects except for minimal glucose intolerance and growth retardation [32, 33]. The last two homologs, IRS5 and -6 also known as DOK4 and DOK5 have poor tissue expression and are poor substrates for the IR [34, 35].

2.3.2 PI3K

PI3K phosphorylates PI, PIP and PIP_2 on the 3-hydroxyl group of the inositol ring. These phosphoinositides control the function and localisation of various effector proteins that bind these lipids via specific lipid-binding domains. PI3K contributes to many processes at cellular level, including cell growth, migration and survival, intracellular vesicular transport and cell cycle progression. There are many isoforms of PI3K which have been grouped into three classes (class I-III) (summary in Table 2.2) based on lipid substrate preferences and structural features. Although the general signalling of PI3K has been elucidated, the specific roles of the different isoforms are still unclear [39]. The class

Table 2.1: **Various IRS isoforms and their expression and functions.**

Isoform	Tissue distribution (protein level)	Function
IRS1	muscle, heart, liver, adipocyte, brain and kidney	glucose homeostasis, primarily involved in muscle metabolism
IRS2	skeletal muscle, adipocyte, lung, brain, liver, kidney, heart and spleen	glucose homeostasis, primarily involved in liver and β cells
IRS3	adipocytes (in rodents, pseudogene in humans)	unknown
IRS4	kidney	unknown
IRS5 (DOK5)	unknown	unknown
IRS6 (DOK6)	unknown	unknown

This table was composed from the following references: [11], [32], [34], [36], [37], [38].

I PI3Ks function as heterodimers consisting of one catalytic subunit (p110α, β, δ or γ) and one regulatory subunit (p85α (or its splice variants p50α and p55α), p85β, p55γ, p84 or p101) [40]. The catalytic subunit is also divided into two classes, class IA (p110α, p110β and p110δ) and class IB (p110γ). The class IA catalytic subunits bind the p85 regulatory subunit type, whereas class IB on the other hand binds two other regulatory subunits, namely, p101 and p84 [41]. The p85 regulatory subunit contains SH2 domains which allows it to bind phosphorylated tyrosines. Binding of p85 to phosphorylated tyrosine residues lifts the p85-mediated inhibition of p110 isoforms bringing them closer to their

Table 2.2: **Various isoforms of PI3K and their functions.**

Classes	Subunit	Type	Tissue distribution
Class I	p85α, p55α, p50α	regulatory	ubiquitous
	p85β		
	p55γ		
	p101		
	p84		
Class IA	p110α	catalytic	ubiquitous
	p110β		
	p110δ		immune cells
Class IB	p110γ		
Class II	PI3KC2α	catalytic	ubiquitous
	PI3KC2β		
	PI3KC2γ		restricted
Class III	VPS34	catalytic	ubiquitous

This table was composed from the following references:[12], [40], [43], [39].

lipid substrates in the membrane [39]. The physiological and signalling roles of the class II PI3Ks are still poorly understood. They were discovered due to their high sequence homology with class I and III PI3Ks. Three isoforms of class II PI3Ks exist in mammals; namely, PI3K-C2α, PI3K-C2β and PI3K-C2γ, of which the first two isoforms are ubiquitously expressed in tissues and the third isoform seems to have more restricted tissue distribution [42]. The third class of PI3Ks contains only one isoform known as VPS34. In mammals, the biological function of VPS34 is thought to involve the regulation of vesicle traffic, including endocytosis, autophagy and phagocytosis [39]. The involvement of class III PI3Ks in signal transduction is yet to be elucidated.

2.3.3 Akt

Akt/PKB are serine/threonine protein kinases that have various regulatory functions, including metabolism of protein, lipids and carbohydrates as well as

control of cell proliferation, growth, survival, apoptosis and angiogenesis [44]. Three isoforms of Akt exist, namely Akt1-3, where Akt1 and Akt2 are highly expressed in skeletal muscle. However, there seems to be two factors that play a role in their specificity for insulin signalling: intracellular localization as well as their relative abundance. Many studies have shown that the Akt2 isoform plays a predominant role in mediating glucose homeostasis, whereas Akt1 and Akt3 are important for growth and brain development respectively [10, 16]. In addition, studies involving murine models have also found that AKT2 KO mice exhibited hyperinsulemia, glucose intolerance, hyperglycemia, and impeded glucose uptake in muscle and adipose tissue, however AKT1 and AKT3 KO mice did not display these traits [45]. Furthermore, *in vitro* studies have also shown a specific mechanism by which Akt2 specifically promotes GLUT4 translocation due to Akt2 being enriched at the plasma membrane in response to insulin. However, this effect was not observed for Akt1 [44, 45]. Recently, it was also demonstrated that GLUT4 translocation is still preserved when the kinase activity of either Akt1 or Akt2 is acutely inhibited. This indicates that both isoforms are sufficient and previous results were based on long term Akt2 depletion and not on catalytic activity. However, Akt1 has been shown to be a necessity for adipogenesis, confirming that some Akt functions require specific isoforms [46].

2.3.4 GLUT4

The transport of glucose is facilitated through a group of solute carriers referred to as the GLUT family. These solute carriers are distributed in various tissues, possess different sugar specificities and have unique kinetic properties. There are 13 members of the GLUT family (GLUT1-12), including a myo-inositol transporter HMIT1 [8]. Four of these transporters, belonging to the class I glucose transporters (GLUT1-4), have been characterised in detail [47]. GLUT1 is responsible for basal glucose uptake and is ubiquitously expressed. GLUT2 is predominantly expressed in β-cells and the liver, and exhibits a low affinity for glucose. GLUT2 together with hexokinase forms part of the glucose sensor. The GLUT3 isoform is expressed in neurons of adults and during fetal development and has a relatively high affinity for glucose [8]. Similar to the other GLUT members, GLUT4 is specific in its tissue distribution and

functionality. GLUT4 is mainly expressed in fat and muscle and is responsible for insulin stimulated glucose uptake [16]. Insulin promotes the translocation of GLUT4 from intracellular storage sites to the plasma membrane through IR and subsequent reactions in the signalling pathway. Insulin is responsible for a number of steps involved in the movement of GLUT4, including the synthesis of GLUT4 containing vesicles as well as the docking and fusion of these vesicles to the plasma membrane [48, 49]. The regulation of these steps happen downstream of Akt and are mediated by different effectors. AS160 is the best described substrate of Akt essential for GLUT4 translocation. The phosphorylation of AS160 via Akt leads to the inactivation of its GAP activity, consequently activating RAB proteins targeted by AS160 [15, 49, 50]. The primary RAB isoform in muscle cells is RAB8a and RAB10 in fat cells. RAB10 has been shown to be responsible for approximately half of insulin's effect on GLUT4 [51–53]. RAB10 elicits its function at a step before vesicle docking, and recently it was demonstrated that RAB10 could be involved in the synthesis of vesicles containing GLUT4 [54]. Therefore, proteins responsible for vesicle docking and fusion are likely to be independent of AS160 and RAB10.

2.4 Insulin resistance and insulin signalling

The mechanisms of regulation for both IR and IRS are very similar. Both are activated by tyrosine phosphorylation and negatively regulated by serine phosphorylation, protein tyrosine phosphatases (PTPs) and ligand-induced downregulation [20]. Several mechanisms of negative regulation exist, one of which is a class of PTPs; namely PTP1B. PTP1B reduces the kinase activity of IR by interacting with the receptor leading to dephosphorylation of important tyrosine residues [20]. *In vivo* KO studies of PTP1B showed enhanced insulin signalling resulting in improved insulin sensitivity [55]. Downregulation of IR function by proteins such as growth factor receptor- bound protein 10 (Grb10), suppressor of cytokine signalling-1 (SOCS1) and SOCS3 and plasma cell membrane glycoprotein-1 (PC1) work through hindering IR crosstalk between IR and IRS or through the modification of IR kinase activity [56]. The SOCS proteins are of interest as they have been implicated in insulin resistance and could contribute to the pathophysiology of diabetes [57].

Another form of negative IR regulation happens at protein level where the receptor undergoes ligand-stimulated internalisation and degradation. This is a common occurrence in insulin resistant or hyperinsulinaemic states such as T2D and obesity [58]. The negative regulation of IRS proteins through serine phosphorylation can be brought about by insulin, cytokines, free fatty acids and other stimuli [59]. IRS1 has multiple serine phosphorylation sites, and generally it would appear that serine phosphorylation is a negative regulator of IRS1. In insulin resistant states serine phosphorylation of IRS1 is increased and this is thought to play a role in insulin resistance. IRS kinases are activated by insulin [60–62], this indicates that there might be a negative feedback loop for the insulin signalling pathway via IRS serine phosphorylation.

It has been shown that the activation of nuclear factor (NF)-$\varkappa$B mediated pathways can inhibit insulin signalling through IRS1 serine phosphorylation. This indicates that IRS serine phosphorylation might be a mechanism of crosstalk between signalling pathways [20, 63]. However, precisely how serine phosphorylation influences the function of IRS1 remains unclear, although it has been suggested that the phosphorylated serine sites interfere with the functional domains in which IRS1 resides [64–67]. Moreover, despite evidence for a strong correlation between serine phosphorylation of IRS1 and insulin resistance the exact mechanisms involved in the pathophysiology of insulin resistance requires further investigation. The significance of phosphorylation of serine sites located on other IRS isoforms also remains understudied, especially the potential regulation this process may have on insulin resistance [20]. Furthermore, expression levels of IRS may also be important for the regulation of this protein. A decrease in IRS1 and IRS2 expression levels has been shown *in vivo* and *in vitro* in hyperinsulinemic states, however the mechanism leading to the downregulation of protein expression levels has not yet been determined. It could be possible that hyperinsulinemia degrades IRS1 and inhibits IRS2 synthesis at transcriptional level [68]. Another possibility might include the ubiquitin-mediated degradation of IRS1 and IRS2 induced by SOCS proteins [69]. Although the mechanisms underlying the decreased levels of IRS proteins are unclear, overall decreases in both IR and IRS levels contribute to the observed insulin resistant and diabetic phenotypes [20, 70].

Several mechanisms are thought to be responsible for the negative regulation of the insulin signalling pathway via PI3K. The ratio between the regula-

tory and catalytic subunits represents one such mechanism [71]. A high ratio of p85 monomers compared to p85-p110 heterodimer, competes for binding to phosphorylated IRS proteins. Therefore a reduction in p85 monomer should increase insulin action as this would allow more p85-p110 heterodimers to bind to phosphotyrosines on IRS. However, this mechanism provides no explanation for negative effects related to the regulatory subunit as overexpression of p50α or p55α did not result in similar decreases of insulin action compared to that of the p85 regulatory subunit [72]. Two other mechanisms are suggested that can possibly explain the full extent of p85 negative regulation. The first proposed mechanism involves the compartmentalisation and or sequestration of PI3K activity [20]. Luo et al. [73] showed that monomeric p85 regulatory subunits, but not isoforms of the regulatory subunit, isolated IRS and PI3K activity into cellular foci that are unable to produce PIP_3. The second mechanism might involve crosstalk between the stress-pathway and p85 subunit, however this will not be discussed here. Negative regulation via p85 regulatory subunit and not via other isoforms of the regulatory subunit, may indicate that structural differences account for functional differences [20].

Various inhibitory molecules such as PH-domain leucine-rich repeat protein phosphatase (PHLPP) and protein phosphatase-2A (PP2A) regulate Akt activity by directly dephosphorylating Akt [74, 75]. Tribbles-3 (TRB3) is also a regulator of Akt and elicits its function through binding unphosphorylated Akt which inhibits its phosphorylation and activation [76]. In fasting mice, an upregulation in TRB3 levels occurs along with increased hepatic glucose outputs when TRB3 is overexpressed. However, insulin sensitivity is improved by RNAi-mediated downregulation of TRB3 [77]. Another feedback mechanism has been suggested for the inhibition of Akt [78]. It involves an inositol pyrophosphate known as diphosphoinositol pentakisphosphate (IP7). IP7 binds to the PH domain of Akt, leading to the inability of PDK-1 to phosphorylate the Thr^{308} site of Akt. This leads to a decrease in insulin stimulated glucose uptake in adipose and muscle tissue [78, 79].

2.5 L6 muscle cells as a model system

Skeletal muscle are among the most important tissues involved in insulin-dependent glucose uptake and is therefore important for maintaining glucose

homeostasis [7]. It is well known that insulin stimulated glucose uptake in muscle cells occur via the translocation of GLUT4 to the plasma membrane [80]. A defect in GLUT4 activity or glucose transport efficiency is also known to result in the phenotype associated with insulin resistance [81]. Therefore, glucose uptake in muscle cells depend on the insulin stimulated translocation of GLUT4, however, the mechanism underlying GLUT4 translocation has remained unclear. Various *in vitro* model systems have been developed to study glucose uptake via GLUT4 in muscle cells. However, most of the established skeletal muscle cell lines have shown little to no insulin response, with rat L6 and mouse C2C12 myotubes being the only two exceptions [82]. Upon insulin stimulation, L6 myotubes seems to display glucose uptake to a greater extent than C2C12 myotubes [83]. This suggests that L6 myotubes might be the best available *in vitro* model system for studying insulin stimulated glucose uptake in muscle cells [84].

2.6 Systems Biology

Advancements in the fields of molecular biology and biochemistry have led to the discovery of complex signaling interactions occurring between intra- and extracellular biomolecules. Cell signaling pathways represent complex networks which involve many shared components that are responsible for controlling cellular responses to environmental changes. Various experimental approaches exist to identify components of signalling networks as well as their biological function. However, understanding how all these components fit together in an integrated manner can prove challenging [85]. A holistic approach to building a better understanding of complex biological systems involves mathematical and computational modelling, which can assist in the interpretation of data and general biological understanding [86].

There are various modelling approaches utilised in cellular biochemistry, however, models incorporating differential equations coincide the best with underlying biochemical rate laws [85]. Ordinary differential equations (ODE) can be used to describe chemical reactions of systems with a large number of molecules. Partial differential equations (PDE) allow the incorporation of spatial gradients [85], and stochastic methods enable the analysis of systems containing a small number of molecules [88]. Spatial and temporal dynamics of

biochemical processes can be modelled in detail using networks of differential equations, which makes it possible to predict the behaviour of a network under varied conditions. The model outputs of ODE- and PDE-based models are largely dependent on the "free" parameter values and the interaction between species needs to be specified beforehand. The estimation of parameters can be a computationally intensive task for which a considerable amount of data is necessary. ODE modeling becomes more complicated as networks expand, which limits models that where initially designed to represent real biological data to a small number of components [85].

2.6.1 Systems biology of the insulin signalling pathway and T2D

Many models exist that describe parts of the insulin signalling pathway, with some mathematical models even attempting to model entire pathways. However, these models often use different modelling approaches, as well as parts of other models that were created in different environments and under various conditions. Some of these models also use parameter values obtained from literature, from various research groups and various cell lines. Previous models have described insulin binding to IR and receptor recycling [89, 90] as well as regulation of GLUT4 in detail [91]. The Sedaghat model [92] is the first model to include signaling intermediates downstream from IR and upstream of GLUT4 and included signalling intermediates IRS, PI3K, PKC-γ and Akt. However, there are certain limitations in this model. The data used to create this model is limited, obtained from different experimental setups and parameter values seems to be chosen "somewhat arbitrarily" [93]. These facts bring into question the validity of the model, and whether its predictions are an accurate representation of the system it is trying to describe. Other groups [94, 95] have used the Sedaghat model [92] as a basis for expanding and including more signalling intermediates, however the results were either not experimentally validated or parameters were either reused or assumed and fitted to a limited data set when compared to the complexity of the model [93].

To our knowledge Brännmark *et al.* [96] were the first to model the insulin signalling pathway in T2D. Their model is ODE based and quantitatively

describes the dynamics of the insulin signalling pathway. All the data were obtained from primary human mature adipocytes from non-diabetic and T2D patients. The model consists of dose-response, time course, and steady state data all obtained from the same cell type. The data was also obtained in a consistent manner which is important for the combination of data for systems analysis. These types of data are important in elucidating complex mechanisms, especially for mathematical modelling. The model was setup in such a way that all the parameters were optimised to fit both the non-diabetic and diabetic state, except for the three diabetic parameters namely: reduced IR concentration, reduced concentration of GLUT4 regulated by IR and lastly, feedback from mTOR in complex with mTORC1. The diabetic parameters were scaled according to the percentage concentration decrease in each of the parameters. Overall they were able to construct a mathematical model of the insulin signalling pathway for both diabetic and non-diabetic states in human adipocytes. Obtaining a model for the non-diabetic state allowed them to identify mechanistic differences in the pathway for the diabetic state. Changes were observed in almost all of the signalling intermediates, but they determined that this was due to the attenuation of a positive feedback mechanism involving mTOR/mTORC1 and IRS1 [96].

Most models that exist on signalling networks are ODE based models. One of the properties of signalling networks are that proteins are involved in more than one reaction and have multiple post-translational modification sites [97]. Creating an ODE based model that can account for all these reactions can become complicated and may be prone to errors. Rule-based models (RBM) are an alternative approach for modelling signalling networks [97, 98]. RBM is based on an assumption that reactions can be grouped together in one "rule" and associated with the same rate law when they involve the same components. The rules specified for a system can then be used to generate ODEs for simulation [99]. Camillo et al. [97] made use of RBM to create a mathematical model integrating three existing models of signalling pathways, namely; PI3K-Akt pathway, the RAS-ERK1/2 pathway and the TSC1/2-mTOR pathway. This model used the Sedaghat model [92] for the PI3K-Akt pathway, which has its own drawbacks as mentioned previously. This model was only partially validated with experimental data of one signalling intermediate for each of the three pathways. However, this might be the first model to account

for the complexities of signalling networks, specifically the insulin signalling pathway. This RBM based model could serve as a useful tool for generating new hypotheses and may allow for the easy inclusion and integration of new mechanisms as they are made available [97].

In summary, there are a variety of models available in literature. These models either describe parts of the insulin signalling pathway or attempt to model the whole pathway with parameters obtained from various sources. To our knowledge, there are no other models that depict the insulin signalling pathway under T2D conditions or in T2D patients, except for Brännmark et al. [96]. Therefore the Brännmark et al. model serves as a starting point for modelling the insulin signalling pathway in both diabetic and non-diabetic states. None of these models link insulin signalling to glucose transport, and we set out to make a core model for insulin signalling linked through to glucose transport.

Chapter 3

Materials and Methods

All abbreviations can be found in the Nomenclature.

Materials: All reagents were obtained from Sigma-Merck unless stated otherwise.

Cell culturing Rat L6 muscle myoblasts were grown in 4.5g/L DMEM supplemented with 10% FBS v/v and incubated at 37°C and 5% CO_2. Cultures were refreshed every two days. When the confluence reached 80% cultures were passaged into multiple flasks and dishes. The cells were subcultured equally into T75 flasks and 100mm culture dishes. Once the cells reached 80% confluence they were differentiated with differentiation media (4g/L DMEM supplemented with 2% v/v HS). Cells were then refreshed every two days with differentiation media until they have developed into myofibers. The differentiated cells were subsequently used in all experiments. Cells were serum starved overnight in 1g/L DMEM and then glucose starved for 3-4 hours with PBS supplemented to 1mM $MgCl_2$ and $CaCl_2$ prior to all experiments (unless stated otherwise). All cell culture photos were taken with an Evos XL Cell Imaging System (Thermo Fisher Scientic).

Insulin Response Assays Insulin (100nM) was added to all the 100mm dishes containing supplemented PBS, and cells were harvested at different time points for time response assays and at different dosages for dose response assays. Dephosphorylation experiments were performed in a similar manner, except the insulin was washed away after 30min and cells were starved for the

respective time points. Cells were harvested by discarding the PBS containing insulin and adding 500µl of 1x lysis buffer (10x Lysis buffer((250mM Tris/HCL pH 7.4, 1.5M NaCl, 1% SDS, 10% Triton X-100)), 1 x phosstop tablet/10mL, 1 x cOmplete EDTA free protease inhibitor tablet/10mL, 10% deoxycholate and MiliQ water) after which the cells were harvested with a scraper and put into Eppendorf tubes. These samples were stored at -80°C for further western blot analyses.

SDS Page and Western Blot Analyses Samples were spun down at 20817 x g for 15min, after which the supernatant was aspirated and aliquoted in new Eppendorf tubes. Laemeli Sample buffer (4x) (Biorad) and Dithiothreitol (DTT) were added in the ratio of (400µl : 100µl) to the supernatant to keep the protein phosphorylation stable. Samples were immediately analysed as to prevent loss of phosphorylated proteins. Samples were loaded on an 8% gel and electrophoresed at 25mA per gel with a 10x SDS Running Buffer. Afterwards the proteins were transferred to a Polyvinylidene fluoride (PVDF) membrane (Biorad) at 20V overnight with a transfer buffer containing 50mM Tris, 380mM Glycine, 0.1% SDS and 20% methanol. Following the transfer, one membrane was used to visualise the total protein and the other mebrane was used to visualise phosphorylated proteins. The membrane was also blocked in 5% fat free milk for two hours before incubation in primary antibody. The membranes were cut at 250kDa, 100kDa, 75kDa and 50kDa respectively and the membrane strips were placed in different primary antibodies overnight at 4°C. After the primary antibody incubation the membrane strips were washed with 1 x TBS-T buffer (100mL 10 x TBS (200mM Tris base and 1.5M NaCl) in 900mL MiliQ with 1mL Tween-20) for 1min, 5min and 15min respectively after which it was incubated for one hour in 1µL secondary antibody: 10mL 5% fat free milk (TBS-T was used to dilute the milk to a concentration of 5%). Following the incubation with secondary antibody, the membranes were washed as before. Blots were visualised using Clarity Western ECL Substrate (Biorad) and the Thermo Scientifiic™ myECL Imager™. ImageJ was used to analyse the western blot images by producing intensity peaks for each band, and then determining the area under the peak. ImageLab™was used to determine normalisation factors from images of the SDS Page gels.

Table 3.1: **A summary of primary- and secondary antibodies used during western blot analyses**

Primary Antibodies	**Ab no**	**Company**
Akt total	9272	Cell Signalling Technology
Akt1 (S473) phos	81283	Abcam
Akt123 (T308) phos	13038	Cell Signalling Technology
Secondary Antibodies		
Anti-Mouse	97023	Abcam
Anti-Rabbit	97051	Abcam

^{14}C glucose transporter activity assays Cells were serum starved overnight in low glucose DMEM and then glucose starved for 3-4 hours with PBS supplemented to 1mM $MgCl_2$ and $CaCl_2$. Cells were pre-incubated with 100nM insulin for 30min. The PBS was aspirated and cells were refreshed with 10mL low glucose DMEM containing 1µCi/mL radiolabelled glucose. After two seconds the media was removed and cells were washed with quenching buffer (cold PBS containing 500mM glucose) twice. Thereafter the cells were harvested with a lysis buffer (50mM Tris, 150mM NaCl and 1% Triton X-100) and 100µl of the sample was added to a vial containing 5mL ScintFlo II and read by Tri-Carb 2810TR Liquid Scintillation Analyzer (PerkinElmer).

Data Analysis and Mathematical Modelling Microsoft Excel and Wolfram Mathematica® were used for all data analysis and modelling. The nonlinearmodelfit function in Wolfram Mathematica® was used to fit for the parameters using the NMinimize method. The timecourse was solved using NDSolve in Wolfram Mathematica®.

Chapter 4

Results

4.1 Introduction

As stated in Chapter 1 we set out to characterise the effects of time and varying insulin doses on the insulin signalling pathway. Tissue culturing and western blot analysis are commonly used to investigate the insulin signalling pathway [15, 100–103]. However, the type of information available in literature is mostly qualitative, i.e. phosphorylated or not, and does not have detail on time and dose response, nor on a mathematical model describing this data. In our opinion, such data and a model are important to compare normal cells with diseased cells, and we therefore set out to characterise a reference model for rat L6 muscle cells.

Initially, our focus was on IR, IRS and Akt as they were the three main nodes identified that lead to the activation of the insulin signalling pathway, resulting in GLUT4 movement to the membrane, but as described in section 4.2.2 we had difficulties quantifying IR and IRS.

In this chapter we present results for the phosphorylation, dephosphorylation and dose-dependent behaviour of Akt Ser^{473} and Thr^{308} in a reference (non-diabetic) state. We use these results to create a model that can describe this behaviour, and that can be used to compare with a model created with data obtained under diabetic conditions. This could lead to insights into the disease mechanisms of insulin resistance and by extension, Type 2 diabetes.

4.2 Optimization of experimental procedures

4.2.1 Cell culturing

In this study the L6 rat skeletal muscle cell line was used for all experiments. The muscle cells were seeded in T75 culturing flasks containing DMEM (1g/L glucose) and initially augmented with 200 g/L glucose to yield a final glucose concentration of 10-11 mM, (medium glucose DMEM) in accordance with a similar protocol developed in a prior study involving C2C12 muscle cells (unpublished work by S. Kuhn). However, this protocol could not be followed for the L6 cells due to the following problems: Cells grew too slow and formed differentiating clusters before reaching confluence, notable quantities of debris were observed under the microscope, the cells also started to dislodge from the culture plates during differentiation (See Fig. 4.1 (a) & (b)). We optimised a growth and differentiation protocol for L6 cells, which included: switching growth medium from DMEM containing ± 10mM glucose to DMEM containing 25mM glucose, seeding in a T25 flask instead of a T75 flask and adjusting the splitting protocol to lower the number of flasks each T75 was split into (see Fig. 4.2). A summary of the changes made to the L6 culturing protocol can be found in table 4.1.

4.2.2 Western blotting

To determine the total- and phosphorylated protein levels of IR, IRS and Akt for L6 cells a protocol developed in our lab for the C2C12 cell line was followed (unpublished work by T. Kouril). Repeating this protocol with L6 samples did not yield the same results. IR provided a smear on the blot using a general anti-phosphotyrosine antibody (abcam # 179530) and did not seem to show a difference between samples unstimulated and stimulated with insulin. Using the same general anti-phosphotyrosine antibody for IRS, multiple bands were observed in the size range of approx. 100 - 250 kDa, making it difficult to acertain which bands were actually IRS. In addition, no insulin response was observed for these samples.

There were no difficulties detecting Akt Ser^{473} phosphorylation with this protocol using anti-AKT1 (phospho S473) antibody (abcam # 81283). However, we were not able to detect bands on the blots for Akt Thr^{308} phosphory-

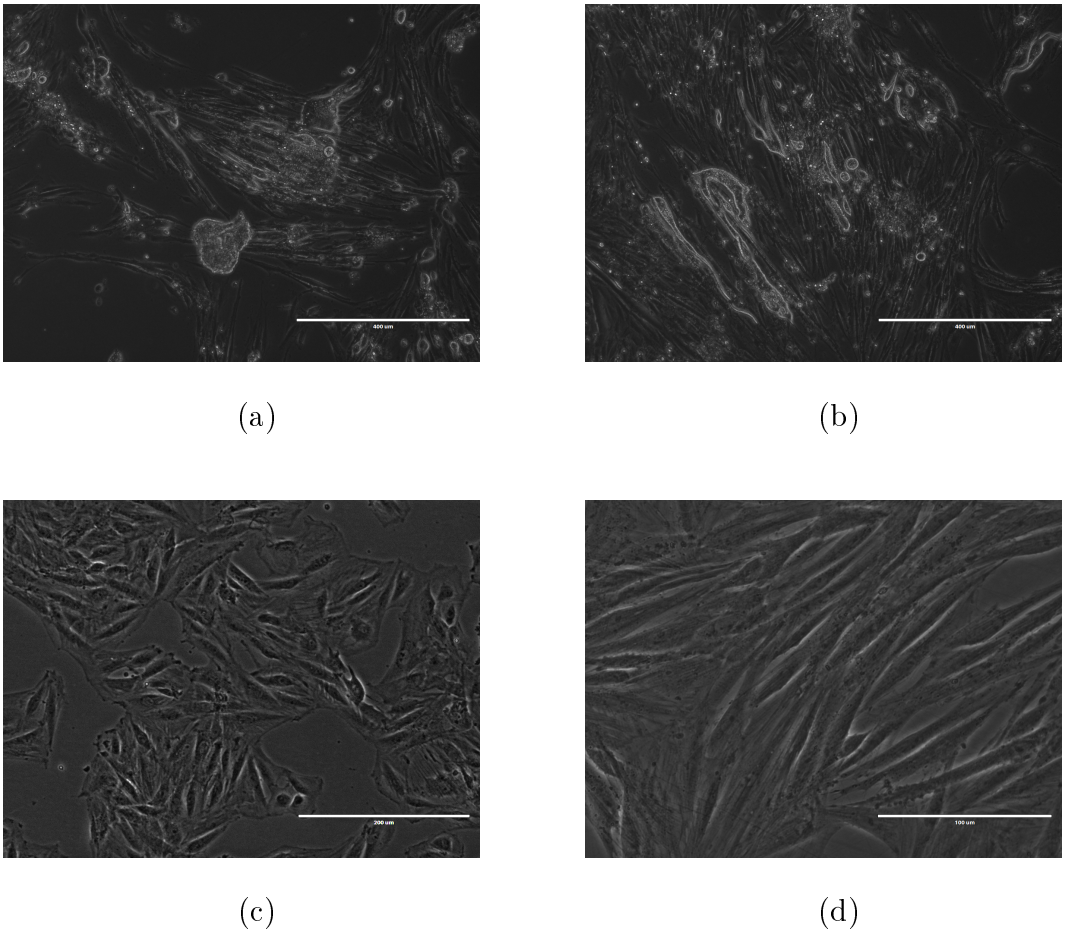

(a) (b)

(c) (d)

Figure 4.1: **Cell culture photos of L6 muscle cells.** Figures (a) and (b) are differentiated L6 muscle fibers that have started lifting off the culture dishes. It can be seen that the fibers appear to be thin and more elongated with notable quantities of cell debris clearly visible. Figure (c) shows growing L6 myoblasts almost ready for differentiation. Figure (d) shows differentiated L6 myofibers, which are formed when myoblasts align and fuse to form thick and long muscle fibers.

lation with the anti-AKT1 (phospho T308) antibody (abcam # 105731). The total protein for IR and Akt were successfully detected, with the total levels remaining constant in all samples, including those stimulated with insulin. IRS total protein, however, also resulted in many different bands but at different sizes compared to the phosphorylated IRS bands, which provided difficulties in identifying which bands were IRS.

To reduce the background for the phosphorylated IR protein we tried using a different primary antibody Anti-Insulin Receptor beta (phospho Y1185)

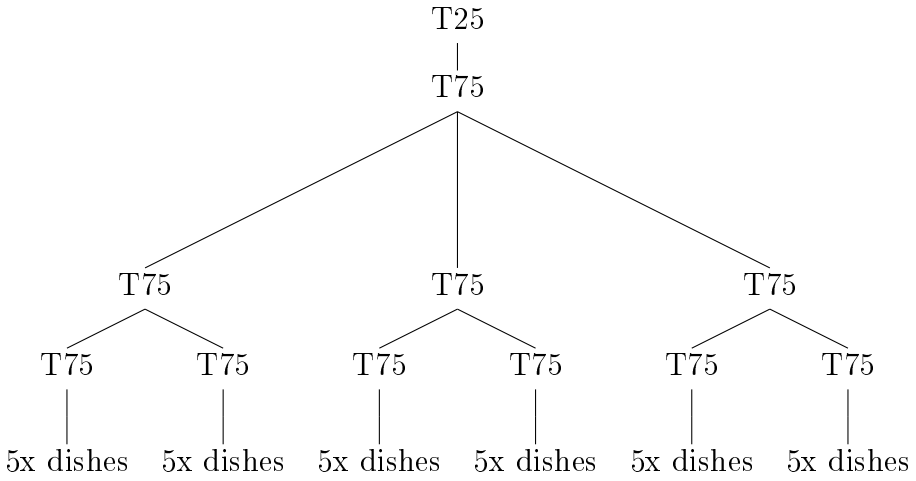

Figure 4.2: **Passaging protocol for L6 myoblasts.** L6 myoblasts were seeded from freezerstock into a T25 flask, once the cells were 70-80% confluent they were passaged into one T75 flask. When the T75 flask reached the same confluence it was split into three T75 flasks. Each of the three T75 flasks were passaged into two T75 flasks, reulting in six T75 flasks. Once these six flasks were 70-80% confluent, they were each passaged into five 100mm cultures dishes respectively.

(abcam # 203278), that is specific for a phosphorylation site on IR (Y1185). This antibody produced an even weaker signal than the first antibody and the smear in the lanes was not cleared up. Another general anti-phosphotyrosine antibody (Cell Signalling Technologies # 9411) was tested and resulted in higher background than the previous general antibody. Adjusting the concentration of the primary antibody (abcam # 179530) from (1:1000 µl) to (1:500 µl) to (1.5:500 µl) did not improve the strength of the signal either. Switching reducing agents from DTT to β-mercaptoethanol (BME) was also unsuccessful in clarifying the smear observed for phosphorylated IR protein. Our last effort was to try and switch membranes from PVDF to nitrocellulose, but this did not reduce the smear. Due to a lack of BSA availability, 5% fat-free milk was used as a blocking agent. However, this did not improve the blots for phosphorylated IR and IRS. None of these changes improved the smear for the phosphorylated IR blots, nor did they improve the ability to distinguish between the various phosphorylated IRS bands (Refer to Appendix A for examples of these results).

This was in stark contrast to phosphorylated AKT Ser^{473} which was always relatively easy to detect. Thus, it was decided to focus on Akt. It is known

Table 4.1: **Summary of L6 culturing conditions:**

Conditions	**C2C12** (unpublished protocol by S. Kuhn)	**L6** (this project)
Seeding	T75 flask	T25 flask
Growth Media	DMEM containing 10-11mM glucose, 10% FBS	DMEM containing 25mM glucose, 10% FBS
Refresh Media	Every two days	Every two days
Initiate differentiation	80-90% confluence	70-80% confluence
Differentiation Media	DMEM containing 25mM glucose, 2% HS	DMEM containing 25mM glucose, 2% HS
Differention time	5-6 days	3-4 days

that both Ser^{473} phosphorylation and Thr^{308} is necessary for full activation of Akt [100], therefore, we attempted to detect the Thr^{308} site once more. A new antibody Phospho-Akt (Thr308) (Cell Signalling Technologies #13038) was used for this attempt, which resulted in the successful detection of the Thr^{308} site. These experimental difficulties limited the number of signal transduction components that could be detected in the L6 cells, but we could still resolve the initial trigger (insulin) and the final output (Akt) for both its phosphorylation sites.

4.3 Measuring Akt Ser^{473} ,Thr^{308} phosphorylation dynamics and GLUT4 transporter activity

In this section we set out to investigate the phosphorylation dynamics of AKT in a time- and dose dependent manner via western blot analysis. Two Akt phosphorylation sites were investigated namely Ser^{473} and Thr^{308} . As far as we know, there is limited information in literature on the time and dose dependent behaviour of any of the signalling intermediates. In this study we attempted to elucidate the time and dose dependent behaviour of both Akt sites.

4.3.1 Akt Ser^{473} and Thr^{308} phosphorylation

L6 muscle cells were grown until fully differentiated, serum and glucose starved, after which they were exposed to 100nM insulin. The dishes were harvested at the indicated time points, and further analysed via western blot. Once the result from the western blots were obtained, ImageJ was used to determine the intensities of the bands, which was normalized with normalization factors obtained from ImageLab™. The normalized intensities were plotted against time to show time dependent phosphorylation for both the Ser^{473} and Thr^{308} site. In Fig. 4.3 (a) there is a relatively fast induction of Ser^{473} phosphorylation compared to Fig. 4.3 (b) which shows a slower induction of Thr^{308} phosphorylation. The total Akt levels (Fig. 4.3 (c)) stay constant with no induction visible between unstimulated and stimulated samples. All levels are expressed relative to the 30min incubation with a 100nM insulin, which was set to 1.

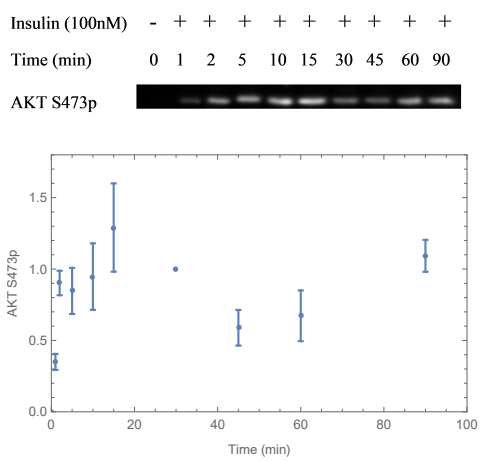

(a)

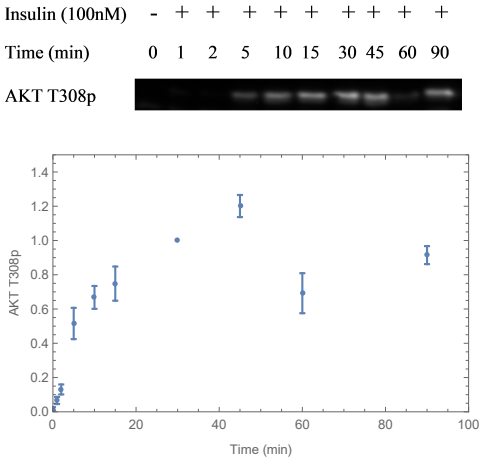

(b)

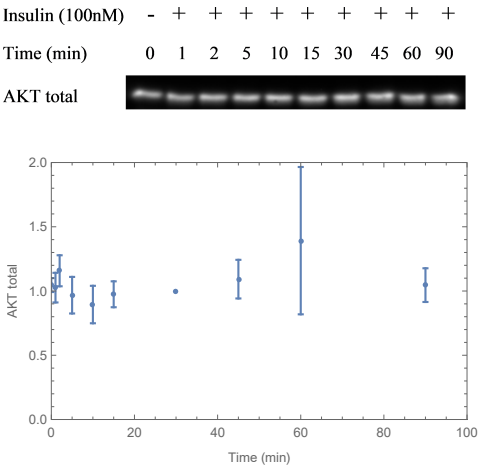

(c)

Figure 4.3: **Time dependent phosphorylation of Akt.** Cells were incubated with 100nM insulin and harvested at different timepoints. Each sample was probed with specific Akt Ser^{473} , Thr^{308} and total antibody. The antibody signal was plotted against time for Akt Ser^{473} (a), Akt Thr^{308} (b) and Akt total (c). Results are means of three experiments ± SE and normalised to the 30min timepoint.

4.3.2 Akt Ser^{473} and Thr^{308} dephosphorylation

To create a model that can acurately describe the time dynamics of Akt phosphorylation, it is important to also investigate the dephosphorylation dynamics of the protein. This experiment was performed similarly to the phosphorylation experiment. L6 muscle cells were grown until fully differentiated, serum and glucose starved, after which they were incubated with 100nM insulin for 30min. After the 30min incubation the cells were washed twice with PBS, and

then incubated with unsupplemented PBS, to determine how fast the Ser^{473} and Thr^{308} site dephosphorylates. In Fig. 4.4 (a) the Ser^{473} site dephosphorylates faster than the Thr^{308} site seen in Fig. 4.4 (b). The total Akt for the dephosphorylation experiment remained constant (Fig. 4.4 (c)) with no decrease in signal when insulin is washed away.

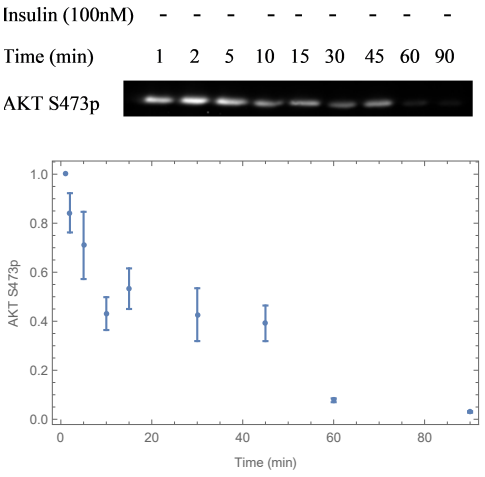

(a)

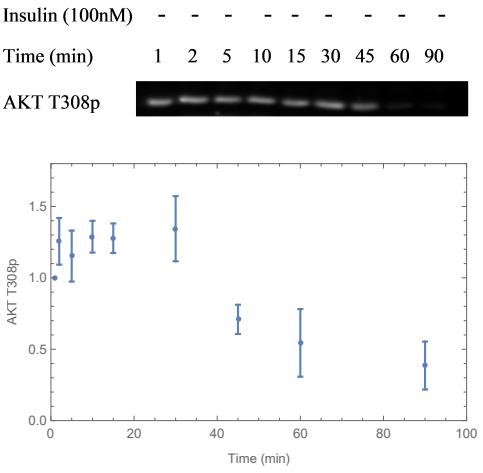

(b)

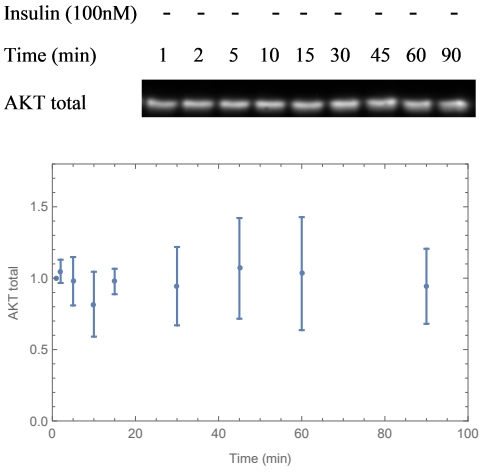

(c)

Figure 4.4: **Time dependent dephosphorylation of Akt.** Cells were incubated with 100nM insulin for 30min after which the insulin was removed at different timepoints and harvested. Each sample was probed with specific Akt Ser^{473} and Thr^{308} antibodies as well as with a total Akt antibody. The antibody signal was plotted against time for Akt Ser^{473} (a), Akt Thr^{308} (b) and Akt total (c). Results are means of three experiments ± SE and normalised to the 1min time point.

4.3.3 Akt Ser^{473} and Thr^{308} dose dependent phosphorylation

The dose dependent behaviour of Akt Ser^{473} and Thr^{308} sites were also investigated by stimulating the cells with different doses of insulin for 30min. The dose response for the Ser^{473} and Thr^{308} site showed similar responses to the various insulin concentrations (as seen in Fig.4.5 (a) and (b)) with a linear increase as insulin concentrations increase. The level of total expression of Akt remained constant with no visible increase in concentration as insulin concentration increased (Fig. 4.5 (c)).

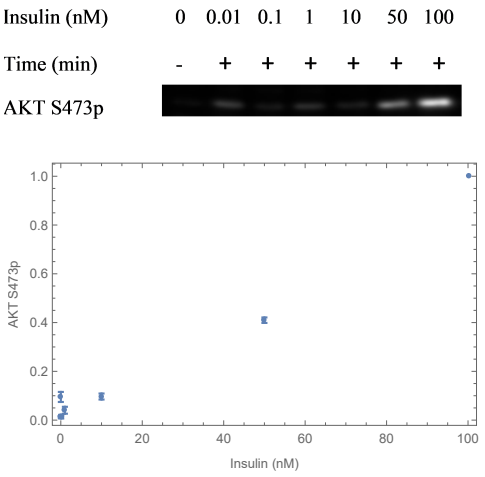

(a)

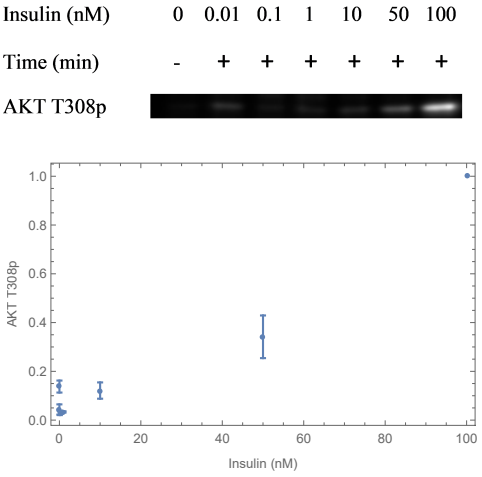

(b)

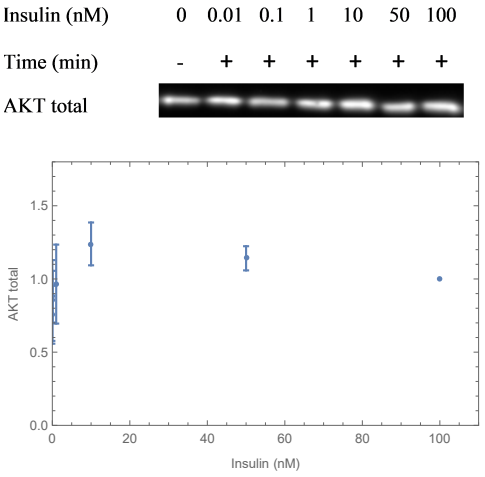

(c)

Figure 4.5: **Dose dependent phosphorylation of Akt.** Cells were incubated with various insulin concentrations and harvested after 30min. Each sample was probed with specific Akt Ser^{473} and Thr^{308} antibodies as well as with a total Akt antibody. The antibody signal was plotted against time for Akt Ser^{473} (a), Akt Thr^{308} (b) and Akt total (c). Results are means of three experiments ± SE and normalised to the 100nM insulin concentration.

4.3.4 GLUT4 transporter activity

A two-second radiolabled glucose assay was performed, as described in chapter 3, to elucidate the transporter behaviour when the cells are stimulated with insulin. Assuming that GLUT1 is constitutively expressed this transporter will be responsible for basal glucose uptake. Upon insulin stimulation GLUT4 will be signalled, via Akt phosphorylation, to translocate to the membrane. Cells were stimulated with 1nM and 100nM insulin for 30min respectively, after which the two-second assay was performed. From Fig. 4.6 it is clear that there is an increase in glucose uptake rate when stimulated with insulin, with a 2x maximal induction when stimulated with 100nM insulin compared to basal uptake. This is similar to what has been reported in literature [104] which found 2-8 fold induction in glucose uptake with acute insulin stimulation.

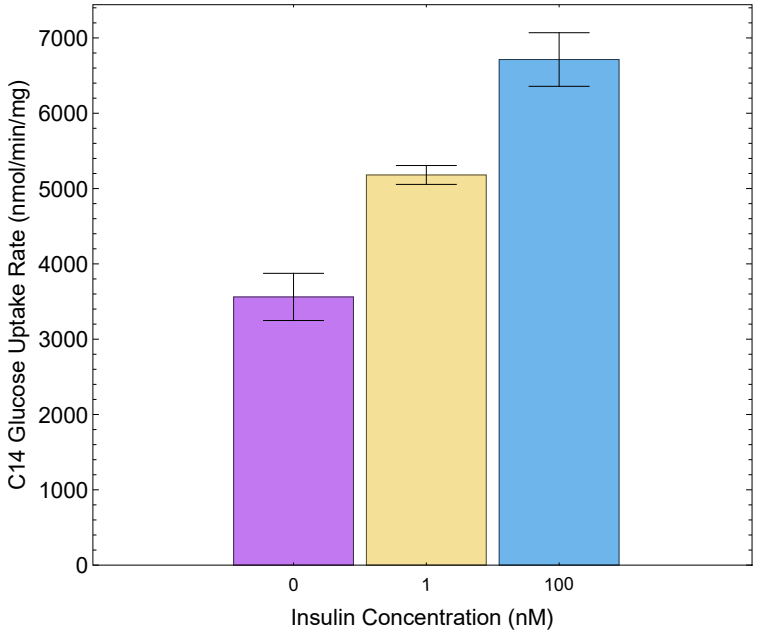

Figure 4.6: **GLUT4 transport activity stimulated with 1nM and 100nM insulin for 30min.** Results are means of three experiments ± SE. Between the control sample (not stimulated with insulin) and the sample stimulated with 1nM insulin there is a 1.46-fold induction ($P<0.05$*). Similarly there is a 1.91-fold ($P<0.05$*) induction between the sample stimulated with a 100nM insulin and the control. It was also determined that there was a 1.29-fold ($P<0.05$*) increase between the sample stimulated with 1nM and 100nM insulin. (*t-test: Two-Sample Assuming Equal Variances)

4.3.5 Summary

We were able to quantify the dose dependent phosphorylation as well as the time dependent phoshorylation and dephosphorylation for both Akt Ser^{473} and Thr^{308} sites. The glucose uptake rate was also determined for two different insulin concentrations. Next we will use the data presented in this section, which was obtained under non-diabetic conditions, to construct a model that can describe the time- and dose dependent behaviour of Akt in response to insulin. For each data set the level of total Akt was determined. In the following section all phosphorylation data sets are normalised to its respective total.

4.4 Modelling the phosphorylation dynamics of Akt Ser^{473} and Thr^{308}

4.4.1 Model Setup

A model was constructed to mathematically describe the time dependent and dose dependent phosphorylation of Akt as a function of insulin. The extent of Akt phosphorylation of the Ser^{473} and Thr^{308} sites, obtained by western blot analyses, was correlated to insulin treatment of differentiated L6 cells. Due to a lack of IR and IRS phosphorylation data, the model directly correlates Akt phosphorylation to insulin action. It is of interest to see whether the model can accurately describe the Akt phosphorylation and dephosphorylation kinetics in the absence of intermediary reactions.

The analysis for Akt Ser^{473} and Thr^{308} are the same and therefore we will show only the equations for the Ser^{473} site. Total Akt can be described as $aktST = aktS(t) + aktSp(t)$ where the unphosphorylated form ($aktS(t)$) and phosphorylated form ($aktSp(t)$) are added to give total Akt ($aktST$). The phosphorylated form $aktSp(t)$ is a dependent variable which is modelled as the total concentration of the component ($aktST$) minus the independent variable ($aktS(t)$).

In the presence of insulin Akt is phosphorylated at a rate of kp and in the absence of insulin Akt is dephosphorylated at a rate of kdp (Fig. 4.7).

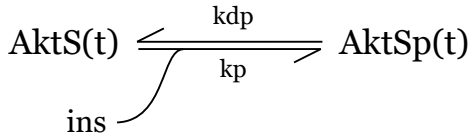

Figure 4.7: **Reaction scheme of the phosphorylation of Akt used for the derivation of kinetic equations.**

We are interested in modelling the appearance of phosphorylated Akt over time ($aktSp(t)$), which can also be described as the dissapearance of the unphosphorylated form of Akt ($aktS(t)$) (Forward reaction in Fig. 4.7. With this information and the reaction scheme we can use mass action kinetics to describe the phosphorylation and dephosphorylation process:

$$\frac{\mathrm{d}aktS(t)}{\mathrm{d}t} = -ins \cdot k_{\mathrm{p_{aktS}}} \cdot aktS(t) + k_{\mathrm{dp_{aktS}}} \cdot (aktSp(t)) \tag{4.4.1}$$

Total Akt ($aktST$) is equal to the sum of the phosphorylated ($aktSp(t)$) and unphosphorylated form of Akt ($aktS(t)$), we can therefore write the following expression:

$$aktSp(t) = (aktST - aktS(t)) \tag{4.4.2}$$

Eq. 4.4.2 can then be substituted into Eq. 4.4.1 to yield the final kinetic description:

$$\frac{\mathrm{d}aktS(t)}{\mathrm{d}t} = -ins \cdot k_{\mathrm{p_{aktS}}} \cdot aktS(t) + k_{\mathrm{dp_{aktS}}} \cdot (aktST - aktS(t)) \tag{4.4.3}$$

4.4.1.1 Using steady state constraints for insulin dose response analysis

To estimate the parameters for the phosphorylation and dephosphorylation we use a dose response experiment to determine steady state phosphorylation

levels. This allows for the estimation of the ratio $\frac{k_{\mathrm{dp_{aktS}}}}{k_{\mathrm{p_{aktS}}}}$ as well as the total amount of Akt ($aktST$). Steady state is assumed to be reached at 30min with an insulin concentration (100nM), and this is normalized to 1. Under steady state the following can be derived for aktS(t):

$$0 = -ins \cdot k_{\mathrm{p_{aktS}}} \cdot aktS(t) + k_{\mathrm{dp_{aktS}}} \cdot (aktST - aktS(t)) \tag{4.4.4}$$

$$\overline{aktS} = \frac{k_{\mathrm{dp_{aktS}}} \cdot aktST}{ins \cdot k_{\mathrm{p_{aktS}}} + k_{\mathrm{dp_{aktS}}}} = \frac{aktST}{ins \cdot \frac{k_{\mathrm{p_{aktS}}}}{k_{\mathrm{dp_{aktS}}}} + 1} \tag{4.4.5}$$

When there is no insulin present ($ins = 0$) then the unphosphorylated form of Akt is equal to the total Akt ($aktS(t) = aktST$), therefore Eq 4.4.5 can be written as:

$$aktST = \frac{aktST}{ins \cdot \frac{k_{\mathrm{p_{aktS}}}}{k_{\mathrm{dp_{aktS}}}} + 1} \tag{4.4.6}$$

Eq 4.4.6 can be simplified to:

$$aktST = 1 + \frac{1}{100} \cdot \frac{k_{\mathrm{dp_{aktS}}}}{k_{\mathrm{p_{aktS}}}} \tag{4.4.7}$$

Eq. 4.4.7 can then be substituted back into Eq.4.4.5 to give an expression for $aktS$:

$$aktS = \frac{1 + \frac{1}{100} \cdot \frac{k_{\mathrm{dp_{aktS}}}}{k_{\mathrm{p_{aktS}}}}}{ins \cdot \frac{k_{\mathrm{p_{aktS}}}}{k_{\mathrm{dp_{aktS}}}} + 1} \tag{4.4.8}$$

Since $aktSp(t)$ is:

$$aktSp(t) = aktST - aktS(t) \tag{4.4.9}$$

Then Eq. 4.4.7 and Eq. 4.4.8 can be substituted into Eq. 4.4.9. This leads to the final equation:

$$\overline{aktSp} = 1 + \frac{1}{100} \cdot \frac{k_{\mathrm{dp_{aktS}}}}{k_{\mathrm{p_{aktS}}}} - \frac{1 + \frac{1}{100} \cdot \frac{k_{\mathrm{dp_{aktS}}}}{k_{\mathrm{p_{aktS}}}}}{ins \cdot \frac{k_{\mathrm{p_{aktS}}}}{k_{\mathrm{dp_{aktS}}}} + 1} \tag{4.4.10}$$

Eq. 4.4.10 will be fitted to a dose response experiment to predict the ratio of $\frac{k_{\mathrm{dp_{aktS}}}}{k_{\mathrm{p_{aktS}}}}$.

The steady state equations were fitted to the experimental data to determine the ratio $\frac{k_{\mathrm{dp_{aktS}}}}{k_{\mathrm{p_{aktS}}}}$ (See Fig. 4.8 and Table 4.2 for parameter estimations). In Fig. 4.8 (a) and (b) the modelfit shows a hyberbolic trend compared to the data which seems to be linear. As the model approaches approximately 0.8, it starts to reach a plateau before the highest tested insulin concentration (100nM).

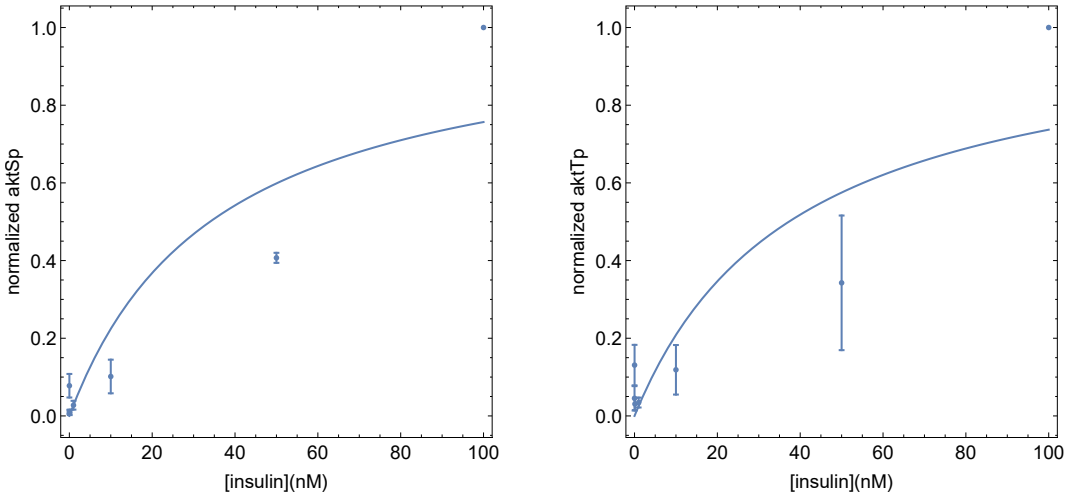

(a) (b)

Figure 4.8: **Model fit to Akt Ser^{473} an Thr^{308} phosphorylation as a function of insulin.** Western blot analysis was used to quantify the phosphorylation levels for both the Ser^{473} and Thr^{308} site. Cells were incubated for 30min with the respective concentrations and values were normalized to 100nM insulin, which was considered steady state phosphorylation. Eq. 4.4.4 was fitted to experimental data for Ser^{473} and Thr^{308} . Data was normalised to their respective total.

4.4.2 Insulin time response

The ratio obtained from the dose response fit (Fig. 4.8 and Table. 4.2) was substituted into Eq. 4.4.3. This equation was then used to simulate both the Ser^{473} and Thr^{308} phosphorylation and dephosphorylation timecourses to determine if the model could describe the experimental data (Fig. 4.3 & 4.4).

Table 4.2: **Kinetic parameters for the steady state rate equations.** Eq. 4.4.10 was fitted to the experimental dose response data for $aktSp(t)$ and $aktTp(t)$

	Estimate	± SE
$\frac{k_{\mathrm{dp_{aktS}}}}{k_{\mathrm{p_{aktS}}}}$	2.78951	0.8799
$aktST$	1.02789	
$\frac{k_{\mathrm{dp_{aktT}}}}{k_{\mathrm{p_{aktT}}}}$	2.55365	0.9298
$aktTT$	1.02553	

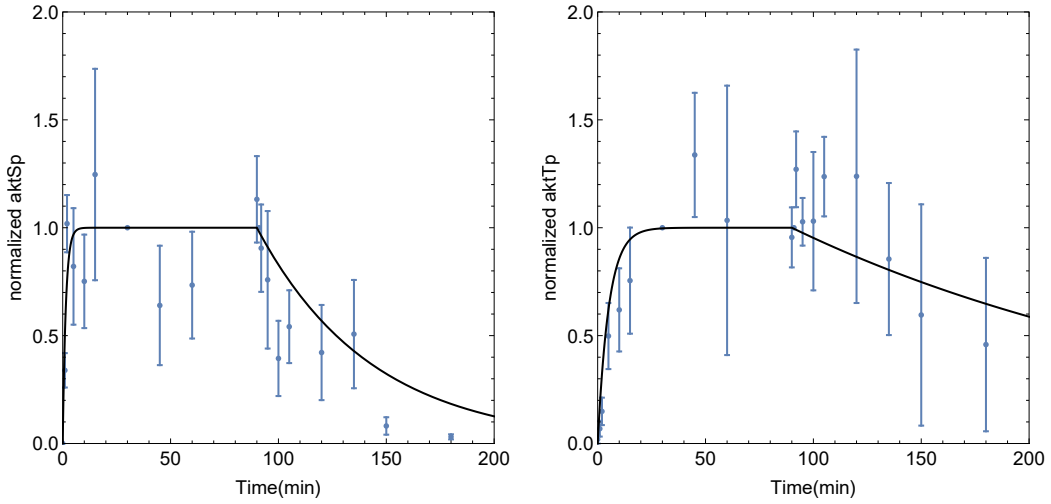

(a) (b)

Figure 4.9: **Phosphorylation and dephosphorylation data for the Ser^{473} (a) and Thr^{308} (b) site shown with the modelfit.** The data was obtained via western blot analyses by stimulating myofibers with a 100nm insulin for the respective time points and then washing away insulin to determine the dephosphorylation. The data is shown in blue with the modelfit shown as a blackcurve.

From Fig. 4.9 it is clear that the model description for the Ser^{473} and Thr^{308} phosphorylation is fairly good, with the phosphorylation of Thr^{308} site being slower compared to the Ser^{473} site. The model was also able to describe the dephosphorylation dynamics of both sites fairly well with the dephosphorylation of the Ser^{473} site being slightly faster than that of the Thr^{308} site. This

could also be determined mathematically by calculating how long it takes for the sites to reach half of the maximal phosphorylation ($t_{\mathrm{p}}0.5$) or dephosphorylation ($t_{\mathrm{dp}}0.5$). The ODE for $aktS(t)$ could be used to determine the time it takes for the phosphorylation of the Ser^{473} site to reach 0.5.

It was determined that $t_{\mathrm{p}}0.5 = 0.99min$ for the Ser^{473} and $t_{\mathrm{p}}0.5 = 3.57min$ for the Thr^{308} site. Therefore, upon insulin stimulation, the Ser^{473} on Akt is phosphorylated 3.6x faster than the Thr^{308} site. To determine the $t_{\mathrm{dp}}0.5$ for both phosphorylation sites the following equation was used:

$$\frac{T}{T_0} = \frac{1}{2} = e^{-\mathrm{kt}_{0.5}} \tag{4.4.11}$$

$$e^{\mathrm{kt}_{0.5}} = 2 \tag{4.4.12}$$

$$k \cdot t_{0.5} = ln2 \tag{4.4.13}$$

$$t_{0.5} = \frac{ln2}{k} \tag{4.4.14}$$

In this case k from Eq. 4.4.14 is kdp for either Akt Ser^{473} or Thr^{308} site. However, we have the estimated ratio for $\frac{k_{\mathrm{dp_{aktS}}}}{k_{\mathrm{p_{aktS}}}}$ and $\frac{k_{\mathrm{dp_{aktT}}}}{k_{\mathrm{p_{aktT}}}}$ (Table 4.2) and now need to determine $k_{\mathrm{dp_{aktS}}}$ and $k_{\mathrm{dp_{aktT}}}$ by substituting estimated values for $k_{\mathrm{p_{aktS}}}$ and $k_{\mathrm{p_{aktT}}}$.

From the model it is estimated that $k_{\mathrm{p_{aktS}}} = 0.0068min^{-1}$ and $k_{\mathrm{p^{aktT}}} = 0.0019min^{-1}$. We can thus calculate that $k_{\mathrm{dp_{aktS}}} = 0.0188min^{-1}$ and $k_{\mathrm{dp_{aktT}}} = 0.00483min^{-1}$. These values can be substituted into Eq. 4.4.14 to calculate $t_{\mathrm{dpS}}0.5 = 36.8min$ and $t_{\mathrm{dpT}}0.5 = 143.5min$. Therefore, upon insulin removal, the Thr^{308} site dephosphorylates 3.8x slower than the Ser^{473} site.

4.4.3 Linking glucose transport to signalling

Akt phosphorylation has been identified as the main component responsible for signalling GLUT4 to translocate from the cytosol ($glutC(t)$) to the membrane [20]. The movement of the transporter to the membrane ($glutM(t)$) was measured through a two-second radiolabelled glucose assay. Mass action kinetics, similar to that of the Ser^{473} and Thr^{308} phosphorylation, was used for linking Akt phosphorylation to glucose transport. If we assume that the total

transporter concentration stays constant then $glutT = glutM(t) + glutC(t)$ and $glutM = glut4 + glutB$. Here $glutB$ represents the basal transport level independent of insulin, leading to the following ODE and steady state relation:

$$\frac{\mathrm{d}glutM(t)}{\mathrm{d}t} = (aktST - aktS(t)) \cdot k_{\mathrm{in}} \cdot (glutT - glutM(t)) - k_{\mathrm{out}} \cdot (glutM(t) - glutB) \tag{4.4.15}$$

$$0 = (aktST - aktS(t)) \cdot k_{\mathrm{in}} \cdot (glutT - glutM(t)) - k_{\mathrm{out}} \cdot (glutM(t) - glutB) \tag{4.4.16}$$

$$\frac{k_{\mathrm{out}}}{k_{\mathrm{in}}} = (aktST - aktS(t)) \cdot \frac{(glutT - glutM(t))}{(glutM(t) - glutB)} \tag{4.4.17}$$

$$glutM(t) \cdot ((aktST - aktS(t)) + \frac{k_{\mathrm{out}}}{k_{\mathrm{in}}}) = (aktST - aktS(t)) \cdot glutT + \frac{k_{\mathrm{out}}}{k_{\mathrm{in}}} \cdot glutB \tag{4.4.18}$$

$$\overline{glutM} = \frac{(aktST - aktS) \cdot glutT + \frac{k_{\mathrm{out}}}{k_{\mathrm{in}}} \cdot glutB}{(aktST - aktS) + \frac{k_{\mathrm{out}}}{k_{\mathrm{in}}}} \tag{4.4.19}$$

With:

$$glutT = (1 + \frac{k_{\mathrm{out}}}{k_{\mathrm{in}}}) \cdot glutM_{\mathrm{max}} - \frac{k_{\mathrm{out}}}{k_{\mathrm{in}}} \cdot glutB \tag{4.4.20}$$

Eq. 4.4.19 and Eq. 4.4.20 was fitted to the dose response data (Fig. 4.5) of Akt Ser^{473} and Thr^{308} phosphorylation and GLUT4 activity (Fig. 4.10). $glutM_{\mathrm{max}}$ was set to 6713.44 nmol/min/mg at a phosphorylation level of 1 for Akt (30min incubation with 100nM insulin) and basal glucose uptake ($glutB$) was set to 3561.12 nmol/min/mg which was the uptake when no insulin was added (Fig. 4.6). The values for $glutM_{\mathrm{max}}$ and $glutB$ were obtained from our dose response experiment in Fig. 4.6.

There is a hyperbolic relationship between glucose transport and phosphorylated Akt Ser^{473} and Thr^{308} as seen in Fig.4.10 (a) and (b). The model fit corresponds well with the experimental data and it seems to be the same for both phosphorylation sites.

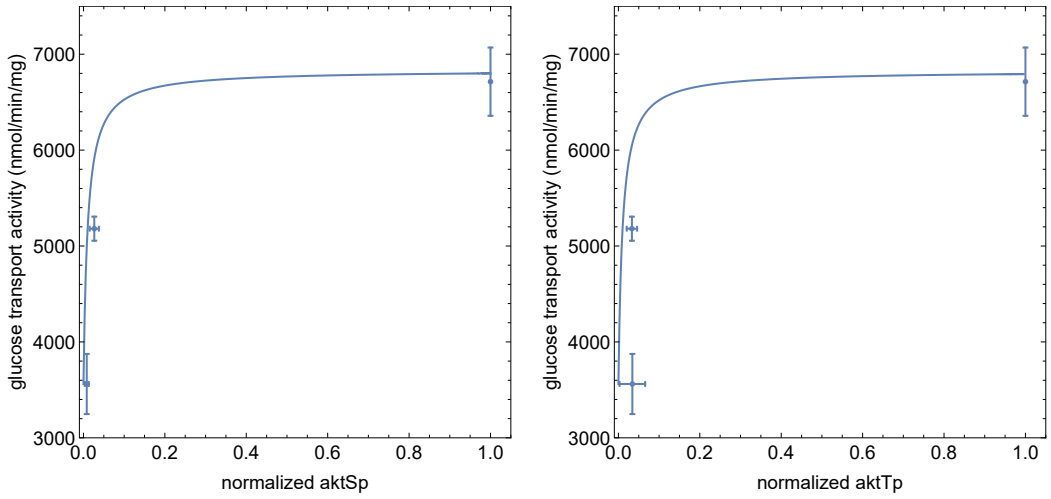

(a) (b)

Figure 4.10: **Glucose transport activity as a function of Akt Ser^{473} (a) and Thr^{308} (b) phosphorylation when stimulated with insulin.** Cells were stimulated with various concentrations of insulin for 30min, Akt Ser^{473} and Thr^{308} phosphorylation were measured via western blot analysis. The phosphorylation levels were normalised to the phosphorylation level obtained with a 100nM insulin. A two-second radiolabelled glucose assay was used to determine the glucose transporter activity.

Chapter 5

Discussion, Future work and Conclusions

5.1 Discussion

T2D is a complicated metabolic disease that involves various organs and biological processes in the body. It is known that T2D patients suffer from hyperglycemia and hyperinsulinemia, but the biochemical processes that lead to these physiological states is still unclear. The main tissues responsible for maintaining glucose homeostasis in the body are muscle cells, adipocytes and the liver. Therefore efforts should be focused on investigating the insulin signalling pathway in these tissues for clarification on the molecular mechanisms that maintain glucose homeostasis. Furthermore, despite numerous studies surrounding the insulin signalling, it remains unclear how the intermediates in the pathway respond to insulin over time or even at higher concentrations of insulin. One method to study these pathway responses would be the construction of mathematical models to predict the outcomes of these changes. Mathematical models can help us understand complex systems and how they fit together, as well as identify possible drug targets. Due to the complexity of the insulin signalling pathway we set out to build a mathematical model that can describe the behaviour of its intermediates over time.

This study focused on characterising the dynamic behaviour of Akt in a time and dose dependent manner as well as investigating the glucose uptake rate in L6 skeletal muscle cells with the ultimate goal of creating a mathemat-

ical model of the reference "healthy" state that can describe this behaviour. It was important during this study to define and optimise the culturing conditions. This was a time consuming process, but was important for ensuring that there was consistency between different culture sets.

Due to the complexity of the insulin signalling pathway we were not able to quantify all of the intermediates of the pathway. However, we were able to quantify the time and dose dependent behaviour of two phosphorylation sites on Akt (Ser^{473} and Thr^{308}) and establish the glucose uptake rate for L6 cells at two different insulin concentrations. The phosphorylation of Akt increased over time for both Ser^{473} and Thr^{308} sites and decreased over time when insulin was removed. This allowed us to determine that the phosphorylation levels reached steady state at 30min when exposed to 100nM insulin. The dose dependent behaviour of both sites was monitored for 30min at various insulin concentrations.

We know that Akt signals GLUT4 to translocate to the membrane where it will import glucose into the cell. In an attempt to link glucose transport to Akt the time and dose dependent behaviour of GLUT4 was also investigated. However, we were not able to determine the time dependent behaviour of GLUT4 and could only determine the rate of glucose uptake at two different insulin concentrations.

Next we used ODEs to create a mathematical model describing the insulin signalling pathway in L6 cells. The model was fitted on the dose response data of the two Akt sites to obtain two parameter ratios, namely; $\frac{k_{\mathrm{dp_{aktS}}}}{k_{\mathrm{p_{aktS}}}}$ & $\frac{k_{\mathrm{dp_{aktT}}}}{k_{\mathrm{p_{aktT}}}}$. The fitted parameters were then used in the model to determine if the model could accurately describe the timecourse data for the Akt sites. The ratio was fitted on the steady state and therefore constrained to the steady state fit (Fig. 4.8).

Even though the model fit for the steady state does not follow the trend of the data accurately, the model was still able to describe the time course data well with the ratio obtained from the steady state fit (Fig. 4.9). We were also interested in determining the difference between the phosphorylation sites when it came to the time it took for each site to become half maximally phosphorylated. We could mathematically determine that the Ser^{473} site phosphorylates 3.6x faster and dephosphorylates 3.8x faster compared to that of the Thr^{308} site.

Next we linked the dose behaviour of Akt to the dose behaviour of GLUT4 by plotting phosphorylated Akt versus GLUT4 uptake rate. The model fit follows the data closely in a hyperbolic manner indicating that as the phosphorylation of Akt increases so does the transporter activity of GLUT4. No difference was found for the steady state relation between AktSp and AktTp and transport activity.

It is well known that insulin is an oscillating hormone, meaning that for a period of time cells are exposed to insulin and a period of time it is not. When insulin binds the IR it sets off a phosphorylation cascade namely the insulin signalling pathway. However, in the absence of insulin these phosphorylated proteins in the cascade are dephosphorylated and are ready to be phosphorylated when the next insulin spike occurs. It would seem that this dephosphorylation would be of importance to investigate, but most studies only look at the phosphorylation state of proteins.

There are mathematical models on signalling pathways for example Kholodenko et al. [105, 106] which include both the phosphorylation and dephosphorylation of certain reactions in their model. In the first model Kholodenko et al.[105] gives a kinetic description of signalling via the Epidermal Growth Factor Receptor (EFGR). In this model they include the dephosphorylation of EFG:EFGR complex. In the second model [106] they give a kinetic description of the mitogen-activated protein kinase (MAPK) cascade including dephosphorylation reactions for MAPK and the MAPK kinases. The EFGR model includes some data for the dephosphorylation, but lacks resolution over time. The dephosphorylation reactions in MAPK model is not based on experimental data. This might be due to the lack of such dephosphorylation data at the time.

It seems like common practice for mathematical models to include dephosphorylation reactions in their kinetic descriptions, however these are not validated by experimental data. This is limiting for models based on ODEs that describe the behaviour of proteins over time, but does not include how these proteins behave when the activating molecule, in our case insulin, is removed. This dephosphorylation behaviour is also important when considering conditions such as insulin resistance and T2D where insulin is present at elevated levels, or omnipresent. As the dissapearance of insulin allows for dephosphorylation to happen, an elevated level or a consistent level of insulin will change

the dynamics of dephosphorylation in the signalling pathway.

One model that does however include dephosphorylation dynamics is the model of Bränmark et al. [96]. As mentioned previously in section 2.6.1 this model made use of adipose tissue obtained from non-diabetic and diabetic subjects, and quantified signalling intermediates of the insulin signalling pathway in a time and dose dependent manner. Their systematic approach allowed them to compare differences between the non-diabetic and diabetic model, leading to their discovery of a feedback mechanism that accounts for the changes observed between the two models, offering a possible mechanism for insulin resistance at a cellular level. We aim to apply a similar approach in muscle cells that could possibly elucidate cellular mechanisms for insulin resistance. In our model setup we would create similar plots to that in Fig. 4.8 and 4.10 for the diabetic state. This will allow us to distinguish between changes in insulin signalling and changes in glucose transport induction between the reference and diabetic state.

In this study we aimed to construct a quantitative description of the insulin signalling pathway and how this is linked to glucose transport by addressing four objectives. Firstly, we investigated the two phosphorylation sites on Akt (Ser^{473} and Thr^{308}) at varying insulin concentrations to determine a dose response for these sites. Secondly, the phosphorylation and dephosphorylation of these two sites were quantified over time. Thirdly, we tested the transport dynamics of GLUT4 over time, but could only quantify the transporter activity for the basal- and stimulated conditions (1nM and 100nM insulin). These data allowed us to address our final aim to construct a mathematical model that describe components of the insulin signalling pathway.

Future research: As mentioned before there are three compartments we are interested in investigating for the model, namely: insulin signalling, glucose transport and glucose metabolism. In this study we only investigated Akt Ser^{473} and Thr^{308} phosphorylation sites and started initial investigations into GLUT4 kinetics for the reference state. Future studies should focus on quantifying the reference state of more intermediates in the insulin signalling pathway, especially those highlighted in chapter 2 as they have been shown to play important roles in the pathway. It is also important to extend the data on GLUT4 to include time course data as well as more resolution on

its dose dependent behaviour as we were not able to elucidate this behaviour in the current study. These components can then be incorporated into the model we created in section 4.4 for the reference state, which could bolster the accuracy of the predictions obtained from the model. Glucose metabolism also needs investigation under reference conditions before moving on to studies in a "diabetic state". The next step should include investigating the insulin signalling intermediates, glucose transport and glucose metabolism under "diabetic" conditions for the purpose of creating a model for the diabetic state. This can be achieved by growing cells in high glucose and insulin. This will hopefully allow us to compare the reference state model with the diabetic state model to identify where the differences lie between the two states.

5.2 Conclusion

Although we were not able to quantify IR and IRS we were able to look at the first and last components of the insulin signalling pathway, insulin and Akt as well as GLUT4. This allowed us to create a quantitative model that could predict the time dependent behaviour of Akt Ser^{473} and Thr^{308} phosphorylation as a function of insulin as well as linking Akt phosphorylation and glucose transport. We found that the model descriptions correlated quite well with the experimental data despite the lack of data on intermediates between insulin and Akt. This model can be used as a starting point for future studies investigating the insulin signalling pathway in both the reference- and diabetic state. To the best of our knowledge this model represents the first attempt to model the reference state of the insulin signalling pathway in L6 muscle cells.

Appendix A

Appendix

IR #179530 (1:1000 primary antibody)

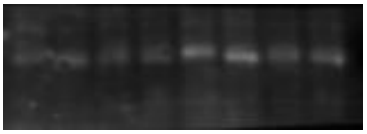

IRS #179530 (1:1000 primary antibody)

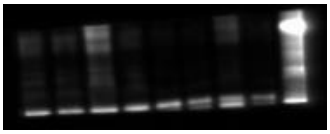

IR #179530 (1:500 primary antibody)

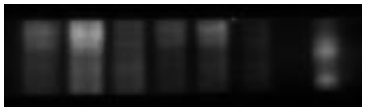

IRS #179530 (1:500 primary antibody)

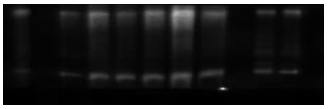

IR #179530 (1.5:500 primary antibody)

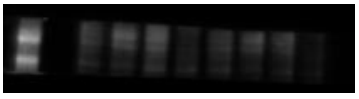

IRS #179530 (1.5:500 primary antibody)

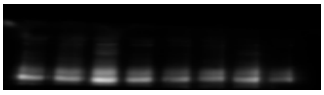

IR #203278

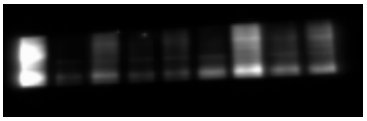

IRS Total #131457

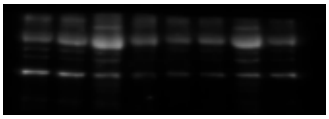

IR #9411

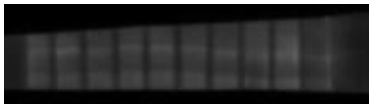

IRS #9411

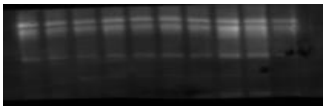

BME as a reducing agent:

IR

IRS

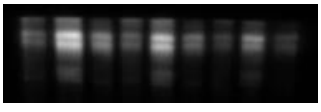

Nitrocellulose membrane:

IR

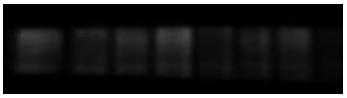

IRS

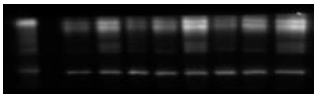

5% Fat free milk:

IR

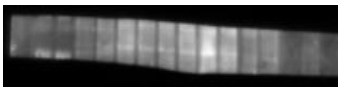

IRS

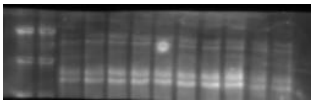

List of References

[1] Ta, S.: Diagnosis and classification of diabetes mellitus. *Diabetes care*, vol. 37, p. S81, 2014.

[2] Organization, W.H. *et al.*: Global report on diabetes. 2016.

[3] Edirs, S., Jiang, L., Xin, X. and Aisa, H.A.: Anti-diabetic effect and mechanism of kursi wufarikun ziyabit in l6 rat skeletal muscle cells. *Journal of pharmacological sciences*, vol. 137, no. 2, pp. 212–219, 2018.

[4] Cusick, M., Meleth, A.D., Agrón, E., Fisher, M.R., Reed, G.F., Knatterud, G.L., Barton, F.B., Davis, M.D., Ferris, F.L., Chew, E.Y. *et al.*: Associations of mortality and diabetes complications in patients with type 1 and type 2 diabetes: early treatment diabetic retinopathy study report no. 27. *Diabetes Care*, vol. 28, no. 3, pp. 617–625, 2005.

[5] Hundal, R.S., Krssak, M., Dufour, S., Laurent, D., Lebon, V., Chandramouli, V., Inzucchi, S.E., Schumann, W.C., Petersen, K.F., Landau, B.R. *et al.*: Mechanism by which metformin reduces glucose production in type 2 diabetes. *Diabetes*, vol. 49, no. 12, pp. 2063–2069, 2000.

[6] Rena, G., Hardie, D.G. and Pearson, E.R.: The mechanisms of action of metformin. *Diabetologia*, vol. 60, no. 9, pp. 1577–1585, 2017.

[7] Saltiel, A.R. and Kahn, C.R.: Insulin signalling and the regulation of glucose and lipid metabolism. *Nature*, vol. 414, no. 6865, p. 799, 2001.

[8] Khan, A. and Pessin, J.: Insulin regulation of glucose uptake: a complex interplay of intracellular signalling pathways. *Diabetologia*, vol. 45, no. 11, pp. 1475–1483, 2002.

[9] Gual, P., Le Marchand-Brustel, Y. and Tanti, J.-F.: Positive and negative regulation of insulin signaling through irs-1 phosphorylation. *Biochimie*, vol. 87, no. 1, pp. 99–109, 2005.

[10] Boucher, J., Kleinridders, A. and Kahn, C.R.: Insulin receptor signaling in normal and insulin-resistant states. *Cold Spring Harbor perspectives in biology*, vol. 6, no. 1, p. a009191, 2014.

[11] Sesti, G., Federici, M., Hribal, M.L., Lauro, D., Sbraccia, P. and Lauro, R.: Defects of the insulin receptor substrate (irs) system in human metabolic disorders. *The FASEB Journal*, vol. 15, no. 12, pp. 2099–2111, 2001.

[12] Fruman, D.A., Meyers, R.E. and Cantley, L.C.: Phosphoinositide kinases. 1998.

[13] Pearce, L.R., Komander, D. and Alessi, D.R.: The nuts and bolts of agc protein kinases. *Nature reviews Molecular cell biology*, vol. 11, no. 1, p. 9, 2010.

[14] Calleja, V., Alcor, D., Laguerre, M., Park, J., Vojnovic, B., Hemmings, B.A., Downward, J., Parker, P.J. and Larijani, B.: Intramolecular and intermolecular interactions of protein kinase b define its activation in vivo. *PLoS biology*, vol. 5, no. 4, p. e95, 2007.

[15] Sano, H., Kane, S., Sano, E., Miinea, C.P., Asara, J.M., Lane, W.S., Garner, C.W. and Lienhard, G.E.: Insulin-stimulated phosphorylation of a rab gtpase-activating protein regulates glut4 translocation. *Journal of Biological Chemistry*, vol. 278, no. 17, pp. 14599–14602, 2003.

[16] Haeusler, R.A., McGraw, T.E. and Accili, D.: Biochemical and cellular properties of insulin receptor signalling. *Nature Reviews Molecular Cell Biology*, vol. 19, no. 1, p. 31, 2018.

[17] Chang, L., Chiang, S.-H. and Saltiel, A.R.: Insulin signaling and the regulation of glucose transport. *Molecular medicine*, vol. 10, no. 7-12, p. 65, 2004.

[18] Furtado, L.M., Somwar, R., Sweeney, G., Niu, W. and Klip, A.: Activation of the glucose transporter glut4 by insulin. *Biochemistry and Cell Biology*, vol. 80, no. 5, pp. 569–578, 2002.

[19] Gavin, J.R., Roth, J., Neville, D.M., De Meyts, P. and Buell, D.N.: Insulin-dependent regulation of insulin receptor concentrations: a direct demonstration in cell culture. *Proceedings of the National Academy of Sciences*, vol. 71, no. 1, pp. 84–88, 1974.

[20] Taniguchi, C.M., Emanuelli, B. and Kahn, C.R.: Critical nodes in signalling pathways: insights into insulin action. *Nature reviews Molecular cell biology*, vol. 7, no. 2, p. 85, 2006.

[21] Becker, A.B. and Roth, R.A.: Insulin receptor structure and function in normal and pathological conditions. *Annual review of medicine*, vol. 41, no. 1, pp. 99–115, 1990.

[22] Sesti, G., Tullio, A., D'Alfonso, R., Napolitano, M., Marini, M., Borboni, P., Longhi, R., Albonici, L., Fusco, A., Agliano, A. *et al.*: Tissue-specific expression of two alternatively spliced isoforms of the human insulin receptor protein. *Acta diabetologica*, vol. 31, no. 2, pp. 59–65, 1994.

[23] Moller, D.E., Yokota, A., Caro, J.F. and Flier, J.S.: Tissue-specific expression of two alternatively spliced insulin receptor mrnas in man. *Molecular Endocrinology*, vol. 3, no. 8, pp. 1263–1269, 1989.

[24] Belfiore, A., Frasca, F., Pandini, G., Sciacca, L. and Vigneri, R.: Insulin Receptor Isoforms and Insulin Receptor/Insulin-Like Growth Factor Receptor Hybrids in Physiology and Disease. *Endocrine Reviews*, vol. 30, no. 6, pp. 586–623, 10 2009.

[25] Araki, E., Lipes, M.A., Patti, M.-E., Brüning, J.C., Haag III, B., Johnson, R.S. and Kahn, C.R.: Alternative pathway of insulin signalling in mice with targeted disruption of the irs-1 gene. *Nature*, vol. 372, no. 6502, p. 186, 1994.

[26] Withers, D.J., Gutierrez, J.S., Towery, H., Burks, D.J., Ren, J.-M., Previs, S., Zhang, Y., Bernal, D., Pons, S., Shulman, G.I. *et al.*: Disruption of irs-2 causes type 2 diabetes in mice. *Nature*, vol. 391, no. 6670, p. 900, 1998.

[27] Miki, H., Yamauchi, T., Suzuki, R., Komeda, K., Tsuchida, A., Kubota, N., Terauchi, Y., Kamon, J., Kaburagi, Y., Matsui, J. *et al.*: Essential role of insulin receptor substrate 1 (irs-1) and irs-2 in adipocyte differentiation. *Molecular and cellular biology*, vol. 21, no. 7, pp. 2521–2532, 2001.

[28] Tseng, Y.-H., Butte, A.J., Kokkotou, E., Yechoor, V.K., Taniguchi, C.M., Kriauciunas, K.M., Cypess, A.M., Niinobe, M., Yoshikawa, K., Patti, M.E. *et al.*: Prediction of preadipocyte differentiation by gene expression reveals role of insulin receptor substrates and necdin. *Nature cell biology*, vol. 7, no. 6, p. 601, 2005.

[29] Huang, C., Thirone, A.C., Huang, X. and Klip, A.: Differential contribution of irs-1 vs irs-2 to insulin signaling and glucose uptake in l6 myotubes. *Journal of Biological Chemistry*, 2005.

[30] Bouzakri, K., Zachrisson, A., Al-Khalili, L., Zhang, B.B., Koistinen, H.A., Krook, A. and Zierath, J.R.: sirna-based gene silencing reveals specialized roles of irs-1/akt2 and irs-2/akt1 in glucose and lipid metabolism in human skeletal muscle. *Cell metabolism*, vol. 4, no. 1, pp. 89–96, 2006.

[31] Laustsen, P.G., Michael, M.D., Crute, B.E., Cohen, S.E., Ueki, K., Kulkarni, R.N., Keller, S.R., Lienhard, G.E. and Kahn, C.R.: Lipoatrophic diabetes in irs1-/-/irs3-/- double knockout mice. *Genes & development*, vol. 16, no. 24, pp. 3213–3222, 2002.

[32] Fantin, V.R., Lavan, B.E., Wang, Q., Jenkins, N.A., Gilbert, D.J., Copeland, N.G., Keller, S.R. and Lienhard, G.E.: Cloning, tissue expression, and chromosomal location of the mouse insulin receptor substrate 4 gene. *Endocrinology*, vol. 140, no. 3, pp. 1329–1337, 1999.

[33] Fantin, V.R., Wang, Q., Lienhard, G.E. and Keller, S.R.: Mice lacking insulin receptor substrate 4 exhibit mild defects in growth, reproduction, and glucose homeostasis. *American Journal of Physiology-Endocrinology And Metabolism*, vol. 278, no. 1, pp. E127–E133, 2000.

[34] Cai, D., Dhe-Paganon, S., Melendez, P.A., Lee, J. and Shoelson, S.E.: Two new substrates in insulin signaling: Irs5/dok4 and irs6/dok5. *Journal of Biological Chemistry*, 2003.

[35] Versteyhe, S., Blanquart, C., Hampe, C., Mahmood, S., Christeff, N., De Meyts, P., Gray, S.G. and Issad, T.: Insulin receptor substrates-5 and-6 are poor substrates for the insulin receptor. *Molecular medicine reports*, vol. 3, no. 1, pp. 189–193, 2010.

[36] White, M.F.: Irs proteins and the common path to diabetes. *American Journal of Physiology-Endocrinology And Metabolism*, vol. 283, no. 3, pp. E413–E422, 2002.

[37] Mardilovich, K., Pankratz, S.L. and Shaw, L.M.: Expression and function of the insulin receptor substrate proteins in cancer. *Cell Communication and Signaling*, vol. 7, no. 1, p. 14, 2009.

[38] Thirone, A.C., Huang, C. and Klip, A.: Tissue-specific roles of irs proteins in insulin signaling and glucose transport. *Trends in Endocrinology & Metabolism*, vol. 17, no. 2, pp. 72–78, 2006.

[39] Vanhaesebroeck, B., Guillermet-Guibert, J., Graupera, M. and Bilanges, B.: The emerging mechanisms of isoform-specific pi3k signalling. *Nature reviews Molecular cell biology*, vol. 11, no. 5, p. 329, 2010.

[40] Jean, S. and Kiger, A.A.: Classes of phosphoinositide 3-kinases at a glance. 2014.

[41] Vanhaesebroeck, B., Leevers, S.J., Panayotou, G. and Waterfield, M.D.: Phosphoinositide 3-kinases: a conserved family of signal transducers. *Trends in biochemical sciences*, vol. 22, no. 7, pp. 267–272, 1997.

[42] Kok, K., Geering, B. and Vanhaesebroeck, B.: Regulation of phosphoinositide 3-kinase expression in health and disease. *Trends in biochemical sciences*, vol. 34, no. 3, pp. 115–127, 2009.

[43] Vanhaesebroeck, B., Ali, K., Bilancio, A., Geering, B. and Foukas, L.C.: Signalling by pi3k isoforms: insights from gene-targeted mice. *Trends in biochemical sciences*, vol. 30, no. 4, pp. 194–204, 2005.

[44] Zheng, X. and Cartee, G.D.: Insulin-induced effects on the subcellular localization of akt1, akt2 and as160 in rat skeletal muscle. *Scientific reports*, vol. 6, p. 39230, 2016.

[45] Gonzalez, E. and McGraw, T.E.: The akt kinases: isoform specificity in metabolism and cancer. *Cell cycle*, vol. 8, no. 16, pp. 2502–2508, 2009.

[46] Kajno, E., McGraw, T.E. and Gonzalez, E.: Development of a new model system to dissect isoform specific akt signaling in adipocytes. *Biochemical Journal*, p. BJ20150191, 2015.

[47] Wood, I.S. and Trayhurn, P.: Glucose transporters (glut and sglt): expanded families of sugar transport proteins. *British journal of nutrition*, vol. 89, no. 1, pp. 3–9, 2003.

[48] Klip, A., Sun, Y., Chiu, T.T. and Foley, K.P.: Signal transduction meets vesicle traffic: the software and hardware of glut4 translocation. *American Journal of Physiology-Cell Physiology*, vol. 306, no. 10, pp. C879–C886, 2014.

[49] Leto, D. and Saltiel, A.R.: Regulation of glucose transport by insulin: traffic control of glut4. *Nature reviews Molecular cell biology*, vol. 13, no. 6, p. 383, 2012.

[50] Ramm, G., Larance, M., Guilhaus, M. and James, D.E.: A role for 14-3-3 in insulin-stimulated glut4 translocation through its interaction with the rabgap as160. *Journal of Biological Chemistry*, vol. 281, no. 39, pp. 29174–29180, 2006.

[51] Ishikura, S., Bilan, P.J. and Klip, A.: Rabs 8a and 14 are targets of the insulin-regulated rab-gap as160 regulating glut4 traffic in muscle cells. *Biochemical and biophysical research communications*, vol. 353, no. 4, pp. 1074–1079, 2007.

[52] Vazirani, R.P., Verma, A., Sadacca, L.A., Buckman, M.S., Picatoste, B., Beg, M., Torsitano, C., Bruno, J.H., Patel, R.T., Simonyte, K. *et al.*: Disruption of adipose rab10-dependent insulin signaling causes hepatic insulin resistance. *Diabetes*, p. db151128, 2016.

[53] Sano, H., Eguez, L., Teruel, M.N., Fukuda, M., Chuang, T.D., Chavez, J.A., Lienhard, G.E. and McGraw, T.E.: Rab10, a target of the as160 rab gap, is required for insulin-stimulated translocation of glut4 to the adipocyte plasma membrane. *Cell metabolism*, vol. 5, no. 4, pp. 293–303, 2007.

[54] Bruno, J., Brumfield, A., Chaudhary, N., Iaea, D. and McGraw, T.E.: Sec16a is a rab10 effector required for insulin-stimulated glut4 trafficking in adipocytes. *J Cell Biol*, pp. jcb–201509052, 2016.

[55] Elchebly, M., Payette, P., Michaliszyn, E., Cromlish, W., Collins, S., Loy, A.L., Normandin, D., Cheng, A., Himms-Hagen, J., Chan, C.-C. *et al.*: Increased insulin sensitivity and obesity resistance in mice lacking the protein tyrosine phosphatase-1b gene. *Science*, vol. 283, no. 5407, pp. 1544–1548, 1999.

[56] Ueki, K., Kondo, T. and Kahn, C.R.: Suppressor of cytokine signaling 1 (socs-1) and socs-3 cause insulin resistance through inhibition of tyrosine phosphorylation of insulin receptor substrate proteins by discrete mechanisms. *Molecular and cellular biology*, vol. 24, no. 12, pp. 5434–5446, 2004.

[57] Emanuelli, B., Peraldi, P., Filloux, C., Chavey, C., Freidinger, K., Hilton, D.J., Hotamisligil, G.S. and Van Obberghen, E.: Socs-3 inhibits insulin signaling and is up-regulated in response to tumor necrosis factor-α in the adipose tissue of obese mice. *Journal of Biological Chemistry*, vol. 276, no. 51, pp. 47944–47949, 2001.

[58] Friedman, J.E., Ishizuka, T., Liu, S., Farrell, C.J., Bedol, D., Koletsky, R.J., Kaung, H.-L. and Ernsberger, P.: Reduced insulin receptor signaling

in the obese spontaneously hypertensive koletsky rat. *American Journal of Physiology-Endocrinology and Metabolism*, vol. 273, no. 5, pp. E1014–E1023, 1997.

[59] Zick, Y.: Ser/thr phosphorylation of irs proteins: a molecular basis for insulin resistance. *Sci. STKE*, vol. 2005, no. 268, pp. pe4–pe4, 2005.

[60] Bouzakri, K., Roques, M., Gual, P., Espinosa, S., Guebre-Egziabher, F., Riou, J.-P., Laville, M., Le Marchand-Brustel, Y., Tanti, J.-F. and Vidal, H.: Reduced activation of phosphatidylinositol-3 kinase and increased serine 636 phosphorylation of insulin receptor substrate-1 in primary culture of skeletal muscle cells from patients with type 2 diabetes. *Diabetes*, vol. 52, no. 6, pp. 1319–1325, 2003.

[61] Harrington, L.S., Findlay, G.M., Gray, A., Tolkacheva, T., Wigfield, S., Rebholz, H., Barnett, J., Leslie, N.R., Cheng, S., Shepherd, P.R. *et al.*: The tsc1-2 tumor suppressor controls insulin–pi3k signaling via regulation of irs proteins. *The Journal of cell biology*, vol. 166, no. 2, pp. 213–223, 2004.

[62] Miller, B.S., Shankavaram, U.T., Horney, M.J., Gore, A.C., Kurtz, D.T. and Rosenzweig, S.A.: Activation of cjun nh2-terminal kinase/stress-activated protein kinase by insulin. *Biochemistry*, vol. 35, no. 26, pp. 8769–8775, 1996.

[63] Cai, D., Yuan, M., Frantz, D.F., Melendez, P.A., Hansen, L., Lee, J. and Shoelson, S.E.: Local and systemic insulin resistance resulting from hepatic activation of ikk-β and nf-κb. *Nature medicine*, vol. 11, no. 2, p. 183, 2005.

[64] Hirosumi, J., Tuncman, G., Chang, L., Görgün, C.Z., Uysal, K.T., Maeda, K., Karin, M. and Hotamisligil, G.S.: A central role for jnk in obesity and insulin resistance. *Nature*, vol. 420, no. 6913, p. 333, 2002.

[65] Aguirre, V., Uchida, T., Yenush, L., Davis, R. and White, M.F.: The c-jun nh2-terminal kinase promotes insulin resistance during association with insulin receptor substrate-1 and phosphorylation of ser307. *Journal of Biological Chemistry*, vol. 275, no. 12, pp. 9047–9054, 2000.

[66] Craparo, A., Freund, R. and Gustafson, T.A.: 14-3-3 (ε) interacts with the insulin-like growth factor i receptor and insulin receptor substrate i in a phosphoserine-dependent manner. *Journal of Biological Chemistry*, vol. 272, no. 17, pp. 11663–11669, 1997.

[67] Bard-Chapeau, E.A., Hevener, A.L., Long, S., Zhang, E.E., Olefsky, J.M. and Feng, G.-S.: Deletion of gab1 in the liver leads to enhanced glucose tolerance and improved hepatic insulin action. *Nature medicine*, vol. 11, no. 5, p. 567, 2005.

[68] Hirashima, Y., Tsuruzoe, K., Kodama, S., Igata, M., Toyonaga, T., Ueki, K., Kahn, C. and Araki, E.: Insulin down-regulates insulin receptor substrate-2 expression through the phosphatidylinositol 3-kinase/akt pathway. *Journal of endocrinology*, vol. 179, no. 2, pp. 253–266, 2003.

[69] Rui, L., Yuan, M., Frantz, D., Shoelson, S. and White, M.F.: Socs-1 and socs-3 block insulin signaling by ubiquitin-mediated degradation of irs1 and irs2. *Journal of Biological Chemistry*, vol. 277, no. 44, pp. 42394–42398, 2002.

[70] Shimomura, I., Matsuda, M., Hammer, R.E., Bashmakov, Y., Brown, M.S. and Goldstein, J.L.: Decreased irs-2 and increased srebp-1c lead to mixed insulin resistance and sensitivity in livers of lipodystrophic and ob/ob mice. *Molecular cell*, vol. 6, no. 1, pp. 77–86, 2000.

[71] Mauvais-Jarvis, F., Ueki, K., Fruman, D.A., Hirshman, M.F., Sakamoto, K., Goodyear, L.J., Iannacone, M., Accili, D., Cantley, L.C. and Kahn, C.R.: Reduced expression of the murine p85α subunit of phosphoinositide 3-kinase improves insulin signaling and ameliorates diabetes. *The Journal of clinical investigation*, vol. 109, no. 1, pp. 141–149, 2002.

[72] Ueki, K., Algenstaedt, P., Mauvais-Jarvis, F. and Kahn, C.R.: Positive and negative regulation of phosphoinositide 3-kinase-dependent signaling pathways by three different gene products of the p85α regulatory subunit. *Molecular and cellular biology*, vol. 20, no. 21, pp. 8035–8046, 2000.

[73] Luo, J., Field, S.J., Lee, J.Y., Engelman, J.A. and Cantley, L.C.: The p85 regulatory subunit of phosphoinositide 3-kinase down-regulates irs-1 signaling via the formation of a sequestration complex. *J Cell Biol*, vol. 170, no. 3, pp. 455–464, 2005.

[74] Brazil, D.P., Yang, Z.-Z. and Hemmings, B.A.: Advances in protein kinase b signalling: Aktion on multiple fronts. *Trends in biochemical sciences*, vol. 29, no. 5, pp. 233–242, 2004.

[75] Gao, T., Furnari, F. and Newton, A.C.: Phlpp: a phosphatase that directly dephosphorylates akt, promotes apoptosis, and suppresses tumor growth. *Molecular cell*, vol. 18, no. 1, pp. 13–24, 2005.

[76] Du, K., Herzig, S., Kulkarni, R.N. and Montminy, M.: Trb3: a tribbles homolog that inhibits akt/pkb activation by insulin in liver. *Science*, vol. 300, no. 5625, pp. 1574–1577, 2003.

[77] Koo, S.-H., Satoh, H., Herzig, S., Lee, C.-H., Hedrick, S., Kulkarni, R., Evans, R.M., Olefsky, J. and Montminy, M.: Pgc-1 promotes insulin resistance in liver through ppar-α-dependent induction of trb-3. *Nature medicine*, vol. 10, no. 5, p. 530, 2004.

[78] Chakraborty, A., Koldobskiy, M.A., Bello, N.T., Maxwell, M., Potter, J.J., Juluri, K.R., Maag, D., Kim, S., Huang, A.S., Dailey, M.J. *et al.*: Inositol pyrophosphates inhibit akt signaling, thereby regulating insulin sensitivity and weight gain. *Cell*, vol. 143, no. 6, pp. 897–910, 2010.

[79] Mackenzie, R.W. and Elliott, B.T.: Akt/pkb activation and insulin signaling: a novel insulin signaling pathway in the treatment of type 2 diabetes. *Diabetes, metabolic syndrome and obesity: targets and therapy*, vol. 7, p. 55, 2014.

[80] Ishiki, M. and Klip, A.: Minireview: recent developments in the regulation of glucose transporter-4 traffic: new signals, locations, and partners. *Endocrinology*, vol. 146, no. 12, pp. 5071–5078, 2005.

[81] Petersen, K.F. and Shulman, G.I.: Etiology of insulin resistance. *The American journal of medicine*, vol. 119, no. 5, pp. S10–S16, 2006.

[82] Nedachi, T. and Kanzaki, M.: Regulation of glucose transporters by insulin and extracellular glucose in c2c12 myotubes. *American Journal of Physiology-Endocrinology and Metabolism*, vol. 291, no. 4, pp. E817–E828, 2006.

[83] Sarabia, V., Ramlal, T. and Klip, A.: Glucose uptake in human and animal muscle cells in culture. *Biochemistry and Cell Biology*, vol. 68, no. 2, pp. 536–542, 1990.

[84] Yap, A., Nishiumi, S., Yoshida, K.-i. and Ashida, H.: Rat l6 myotubes as an in vitro model system to study glut4-dependent glucose uptake stimulated by inositol derivatives. *Cytotechnology*, vol. 55, no. 2-3, pp. 103–108, 2007.

[85] Morris, M.K., Saez-Rodriguez, J., Sorger, P.K. and Lauffenburger, D.A.: Logic-based models for the analysis of cell signaling networks. *Biochemistry*, vol. 49, no. 15, pp. 3216–3224, 2010.

[86] Kestler, H.A., Wawra, C., Kracher, B. and Kühl, M.: Network modeling of signal transduction: establishing the global view. *Bioessays*, vol. 30, no. 11-12, pp. 1110–1125, 2008.

[87] Aldridge, B.B., Burke, J.M., Lauffenburger, D.A. and Sorger, P.K.: Physicochemical modelling of cell signalling pathways. *Nature cell biology*, vol. 8, no. 11, p. 1195, 2006.

[88] Raj, A. and van Oudenaarden, A.: Nature, nurture, or chance: stochastic gene expression and its consequences. *Cell*, vol. 135, no. 2, pp. 216–226, 2008.

[89] Quon, M.J. and Campfield, L.A.: A mathematical model and computer simulation study of insulin receptor regulation. *Journal of theoretical biology*, vol. 150, no. 1, pp. 59–72, 1991.

[90] Wanant, S. and Quon, M.J.: Insulin receptor binding kinetics: modeling and simulation studies. *Journal of theoretical Biology*, vol. 205, no. 3, pp. 355–364, 2000.

[91] Quon, M.J. and Campfield, L.A.: A mathematical model and computer simulation study of insulin sensitive glucose transporter regulation. *Journal of theoretical biology*, vol. 150, no. 1, pp. 93–107, 1991.

[92] Sedaghat, A.R., Sherman, A. and Quon, M.J.: A mathematical model of metabolic insulin signaling pathways. *American Journal of Physiology-Endocrinology and Metabolism*, vol. 283, no. 5, pp. E1084–E1101, 2002.

[93] Nyman, E., Cedersund, G. and Strålfors, P.: Insulin signaling–mathematical modeling comes of age. *Trends in Endocrinology & Metabolism*, vol. 23, no. 3, pp. 107–115, 2012.

[94] Giri, L., Mutalik, V.K. and Venkatesh, K.: A steady state analysis indicates that negative feedback regulation of ptp1b by akt elicits bistability in insulin-stimulated glut4 translocation. *Theoretical Biology and Medical Modelling*, vol. 1, no. 1, p. 2, 2004.

[95] Vinod, P.K.U. and Venkatesh, K.V.: Quantification of the effect of amino acids on an integrated mtor and insulin signaling pathway. *Molecular BioSystems*, vol. 5, no. 10, pp. 1163–1173, 2009.

[96] Brännmark, C., Nyman, E., Fagerholm, S., Bergenholm, L., Ekstrand, E.-M., Cedersund, G. and Strålfors, P.: Insulin signaling in type 2 diabetes experimental and modeling analyses reveal mechanisms of insulin resistance in human adipocytes. *Journal of Biological Chemistry*, vol. 288, no. 14, pp. 9867–9880, 2013.

[97] Di Camillo, B., Carlon, A., Eduati, F. and Toffolo, G.M.: A rule-based model of insulin signalling pathway. *BMC systems biology*, vol. 10, no. 1, p. 38, 2016.

[98] Danos, V., Feret, J., Fontana, W., Harmer, R. and Krivine, J.: Rule-based modelling of cellular signalling. In: *International conference on concurrency theory*, pp. 17–41. Springer, 2007.

[99] Smith, A.M., Xu, W., Sun, Y., Faeder, J.R. and Marai, G.E.: Rulebender: integrated modeling, simulation and visualization for rule-based intracellular biochemistry. *BMC bioinformatics*, vol. 13, no. 8, p. S3, 2012.

[100] Sarbassov, D.D., Guertin, D.A., Ali, S.M. and Sabatini, D.M.: Phosphorylation and regulation of akt/pkb by the rictor-mtor complex. *Science*, vol. 307, no. 5712, pp. 1098–1101, 2005.

[101] Cozzone, D., Fröjdö, S., Disse, E., Debard, C., Laville, M., Pirola, L. and Vidal, H.: Isoform-specific defects of insulin stimulation of akt/protein kinase b (pkb) in skeletal muscle cells from type 2 diabetic patients. *Diabetologia*, vol. 51, no. 3, pp. 512–521, 2008.

[102] Karlsson, H.K., Zierath, J.R., Kane, S., Krook, A., Lienhard, G.E. and Wallberg-Henriksson, H.: Insulin-stimulated phosphorylation of the akt substrate as160 is impaired in skeletal muscle of type 2 diabetic subjects. *Diabetes*, vol. 54, no. 6, pp. 1692–1697, 2005.

[103] Lee, J., Miyazaki, M., Romeo, G.R. and Shoelson, S.E.: Insulin receptor activation with transmembrane domain ligands. *Journal of Biological Chemistry*, pp. jbc–M114, 2014.

[104] Rudich, A. and Klip, A.: Push/pull mechanisms of glut4 traffic in muscle cells. *Acta physiologica Scandinavica*, vol. 178, no. 4, pp. 297–308, 2003.

[105] Kholodenko, B.N., Demin, O.V., Moehren, G. and Hoek, J.B.: Quantification of short term signaling by the epidermal growth factor receptor. *Journal of Biological Chemistry*, vol. 274, no. 42, pp. 30169–30181, 1999.

[106] Kholodenko, B.N.: Negative feedback and ultrasensitivity can bring about oscillations in the mitogen-activated protein kinase cascades. *European journal of biochemistry*, vol. 267, no. 6, pp. 1583–1588, 2000.